

**FEASIBILITY STUDY OF
UPSCALING OXIDATION OF DILUTED
PALM OIL MILL EFFLUENT**

OOI KAI CHUEN

UNIVERSITI TUNKU ABDUL RAHMAN

**FEASIBILITY STUDY OF UPSCALING OXIDATION OF
DILUTED PALM OIL MILL EFFLUENT**

OOI KAI CHUEN

**A project report submitted in partial fulfilment of the
requirements for the award of the degree of
Bachelor of Civil Engineering (Environmental) with Honours**

**Faculty of Engineering and Green Technology
Universiti Tunku Abdul Rahman**

May 2024

DECLARATION

I hereby declare that this project report is based on my original work except for citations and quotations which have been duly acknowledged. I also declare that it has not been previously and concurrently submitted for any other degree or award at UTAR or other institutions.

Signature :



Name : Ooi Kai Chuen

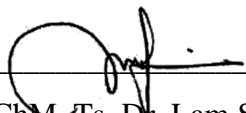
ID No. : 19AGB01580

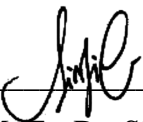
Date : 3rd May 2024

APPROVAL FOR SUBMISSION

I certify that this project report entitled “**FEASIBILITY STUDY OF UPSCALING OXIDATION OF DILUTED PALM OIL MILL EFFLUENT**” was prepared by **OOI KAI CHUEN** has met the required standard for submission in partial fulfilment of the requirements for the award of Bachelor of Civil Engineering (Environmental) with Honours at Universiti Tunku Abdul Rahman.

Approved by,

Signature : 
Supervisor : ChM. Ts. Dr. Lam Sze Mun
Date : 3rd May 2024

Signature : 
Co-Supervisor : ChM. Ts. Dr. Sin Jin Chung
Date : 3rd May 2024

The copyright of this report belongs to the author under the terms of the copyright Act 1987 as qualified by Intellectual Property Policy of Universiti Tunku Abdul Rahman. Due acknowledgement shall always be made of the use of any material contained in, or derived from, this report.

© 2024, Ooi Kai Chuen. All right reserved.

ACKNOWLEDGEMENTS

This research project was accomplished with the invaluable contributions of many individuals. First and foremost, I am sincerely grateful to my research supervisor, ChM. Ts. Dr. Lam Sze Mun, for her patience, guidance, advice, and steadfast support throughout the final year project process. I also appreciate my co-supervisor, ChM. Ts. Dr. Sin Jin Chung, consistently supporting and guiding me.

I am deeply thankful to my senior students, specifically Lim Khar Lok and Wong Xuet Wei, for their helpful advice in using laboratory equipment and instruments. They were always incredibly kind and willing to assist me during the research journey. I am also grateful to the university lab officers, who diligently fulfilled all my laboratory requests.

Finally, I would like to thank my family for their unconditional love and the physical and emotional support they provided me in completing this final year research project. This endeavour was achievable with their belief in my abilities.

FEASIBILITY STUDY OF UPSCALING OXIDATION OF DILUTED PALM OIL MILL EFFLUENT

ABSTRACT

The yearly palm oil production in Malaysia has been rising, contributing to environmental damage from improper disposal of palm oil mill effluents (POME) brought on by inadequate treatment. As a result, the Department of Environment Malaysia and the Malaysian Palm Oil Board wish to strengthen the biochemical oxygen demand (BOD) discharged limit from 100 to 20 ppm. This study proposed UV/H₂O₂ advanced oxidation technology as a tertiary treatment for treated POME to reduce its BOD to 20 ppm. The optimum concentration of H₂O₂ and optimum number of UV lights for UV/H₂O₂ treatment on the POME degradation was determined on a laboratory scale. At the laboratory scale, the UV/H₂O₂ system utilising 400 ppm of H₂O₂ and two UV lights has exhibited exceptional performance, achieving 72.3% colour removal efficiency after 6 hours of treatment. Meanwhile, the best UV/H₂O₂ system performance was yielded in the upscaling experiment under optimal H₂O₂ concentration with pulse dosing and an optimum number of UV lights to assess its feasibility for industrial application. The upscaling UV/H₂O₂ treatment with optimum parameters could reduce POME's BOD from 100 ppm to 15 ppm, resulting in 88.4% colour removal efficiency. The UV/H₂O₂ treatment, during the first three hours in dark conditions, was carried out to determine its feasibility in reducing the BOD of POME to below 20 ppm while saving the cost of treatment. Based on the cost analysis, the UV/H₂O₂ system working as a post-treatment for POME degradation was economically viable. Subsequently, the phytotoxicity was shown to have decreased in the trials using mung bean seeds. By implementing effective and sustainable POME post-treatment technology, these findings helped to improve the sustainability standards and the financial sustainability of palm oil.

TABLE OF CONTENTS

DECLARATION	iii
APPROVAL FOR SUBMISSION	iv
ACKNOWLEDGEMENTS	vi
ABSTRACT	vii
TABLE OF CONTENTS	viii
LIST OF TABLES	xi
LIST OF FIGURES	xiii
LIST OF SYMBOLS / ABBREVIATIONS	xv

CHAPTER

1	INTRODUCTION	1
	1.1 Utilizing Advanced Oxidation Process for Diluted Palm Oil Mill Effluent Treatment	1
	1.2 Problem Statements	4
	1.3 Aims and Objectives	6
	1.4 Scope of Study	7
2	LITERATURE REVIEW	8
	2.1 Review of the Effluent Derived from Palm Oil Industry	8
	2.2 Conventional Treatment for POME	11
	2.3 Advanced Oxidation Processes (AOPs)	15
	2.4 UV Based of AOPs	18
	2.5 Mechanisms of Pollutant Degradation in UV/H ₂ O ₂	21
	2.6 Effect of Operating Parameters	24

2.6.1	Concentration of H ₂ O ₂	24
2.6.2	UV Light and Its Intensity	27
2.7	Kinetic Model of UV/H ₂ O ₂ System	30
2.8	Summary of Literature Review	31
3	METHODOLOGY	32
3.1	Flowchart of Research Methodology	32
3.2	Chemicals and Materials	34
3.3	Experimental Setup	36
3.4	Colour and BOD Test	38
3.5	Parameter Studies	40
3.5.1	UV Irradiance	40
3.5.2	H ₂ O ₂ Dosage Ways	40
3.6	Upscaling UV/H ₂ O ₂ System	41
3.7	Determination of Excess H ₂ O ₂ using Redox Titration	43
3.8	Phytotoxicity Test	44
4	RESULTS AND DISCUSSION	45
4.1	Control Experiment	46
4.2	Effect of Operating Parameter in Lab Scale UV/H ₂ O ₂ Treatment	48
4.2.1	Hydrogen Peroxide Concentration	48
4.2.2	Number of UV Light	50
4.3	Effect of Operating Parameter in Upscaling UV/H ₂ O ₂ Treatment	52
4.3.1	Number of UV Light	52
4.3.2	One-time Dosing vs Pulse Dosing of H ₂ O ₂	54
4.3.3	Pulse Dosing of H ₂ O ₂ vs Pulse Dosing of H ₂ O ₂ with 3 Hours Dark	57
4.4	Determination of Excess H ₂ O ₂	60
4.5	Cost Analysis	62
4.6	Phytotoxicity Evaluation	64

5	CONCLUSION AND RECOMMENDATIONS	66
5.1	Conclusion	66
5.2	Recommendations for Future Studies	67
	REFERENCES	68

LIST OF TABLES

TABLE	TITLE	PAGE
Table 2.1:	Characteristics of Palm Oil Mill Effluent from Previous Case Studies	9
Table 2.2:	Standard Discharge Limits of POME Final Discharge Set by DOE	14
Table 2.3:	Standard Reduction Potential for Different Oxidants (Cuerda-Correa, Alexandre-Franco, and Fernández-González, 2019)	16
Table 2.4:	Rate Constants (k in $M^{-1}s^{-1}$) for Ozone and Hydroxyl Radical Reactions with Different Organic Compounds (Litter, 2005)	17
Table 2.5:	Major Methods for Organics Removal during Wastewater Treatment by Various AOPs (Deng and Zhao, 2015)	18
Table 2.6:	Comparison of The Removal Efficiency of One-Time Dosing versus Pulse Dosing for Various Oxidants	26
Table 2.7:	Various Types of UV Light and Their Applications in Photochemical AOTs (Litter, 2005)	27
Table 2.8:	Comparison of The Removal Efficiency for Different Numbers of UV Lamps and Their Intensities	29
Table 3.1:	Inventory of Chemicals and Materials	35
Table 4.1:	A Summary of the Analysed Quality Parameters of Diluted POME Prior to UV/H ₂ O ₂ Treatment for Degradation Before and After Photolysis Under UVC Light with Hydrogen Peroxide Oxidant ([POME] = 100 ppm, [H ₂ O ₂] = 400 ppm, Pulse Dosing Rate = 0.3333 mL/min, UVC Light Irradiation Time = 12 hours)	59

Table 4.2: Cost and Total Electricity Used for the UV/H ₂ O ₂ System	62
Table 4.3: Total Cost of Material for POME Degradation by UV/H ₂ O ₂ System	63

LIST OF FIGURES

FIGURE	TITLE	PAGE
Figure 2.1:	Reaction mechanisms for UV/H ₂ O ₂ system (Legrini, Oliveros, and Braun, 1993)	21
Figure 3.1:	Flowchart of Overall Experimental Work	33
Figure 3.2:	Schematic Diagram of UV/H ₂ O ₂ System	37
Figure 3.3:	Experimental Setup of UV/H ₂ O ₂ System at Laboratory Scale	37
Figure 3.4:	Schematic Diagram of Upscaling UV/H ₂ O ₂ System	42
Figure 3.5:	Side View of Upscaling UV/H ₂ O ₂ System	42
Figure 3.6:	Redox Titration with Standard KMnO ₄ solution	43
Figure 4.1:	BOD Reduction and Colour Removal Efficiency of POME for The Various Conditions of Control Experiment	47
Figure 4.2:	Effect of Different Concentrations of H ₂ O ₂ on POME with One UV Light ([POME] = 100 mg/L, [H ₂ O ₂] = 400 mg/L)	48
Figure 4.3:	Decolourization Efficiency of POME at Various Numbers of UV Lights with One-time Dosing of H ₂ O ₂ ([POME] = 100 mg/L, [H ₂ O ₂] = 400 mg/L)	50
Figure 4.4:	BOD Reduction of POME at Different Numbers of UV Lights with One-time Dosing of H ₂ O ₂ ([POME] = 100 mg/L, [H ₂ O ₂] = 400 mg/L)	53
Figure 4.5:	BOD Reduction of POME at Different Dosing Methods with 2 UV Lights ([POME] = 100 mg/L, [H ₂ O ₂] = 400 mg/L, Pulse Dosing Rate = 0.3333 mL/min)	55

- Figure 4.6: Pseudo-First-Order Kinetics Plot of POME Degradation During UV/H₂O₂ Process with Different Dosing Methods ([POME] = 100 mg/L, [H₂O₂] = 400 mg/L, Pulse Dosing Rate = 0.3333 mL/min) 56
- Figure 4.7: BOD Reduction of POME at Different Conditions of Pulse Dosing with 2 UV Lights ([POME] = 100 mg/L, [H₂O₂] = 400 mg/L, Pulse Dosing Rate = 0.3333 mL/min) 57
- Figure 4.8: Amount of H₂O₂ in Excess in POME Solution after 12 hours of UV/H₂O₂ Treatment ([POME] = 100 mg/L, [H₂O₂] = 400 mg/L, Pulse Dosing Rate = 0.3333 mL/min) 60
- Figure 4.9: Phytotoxicity tests of POME before and after UV/H₂O₂ Treatment 64
- Figure 4.10: Mung Bean Seeds Germination after 12 days: (a) Control (Tap Water); (b) Before Treatment (Untreated POME); (c) After Treatment (Treated POME) 65

LIST OF SYMBOLS / ABBREVIATIONS

$^{\circ}\text{C}$	Degree Celsius
eV	Electron Volt
kWh	Kilowatt-Hour
M	Molar
mM	Millimolar
mW	Milliwatts
nm	Nanometre
ppb	Parts Per Billion
ppm	Parts Per Million
RM	Ringgit Malaysia
V	Volt
W	Watt
Ω	Ohm
BOD_0	Initial Biochemical Oxygen Demand Value of POME
BOD_t	Final Biochemical Oxygen Demand Value of POME
C_0	Initial POME Concentration Value
C_t	Final POME Concentration Value
DO_0	Initial Dissolved Oxygen Value
DO_3	Final Dissolved Oxygen Value After 3 Days Incubation
E_0	Oxidation/Reduction Potential
e^-_{cb}	Conduction Band
h_ν	Light Energy
$h_\nu^+_{vb}$	Valence Band
k'	Rate Constant
L_c	Radicle Length of Control
L_s	Radicle Length of Sample

P	Dilution factor
R^2	Coefficient of Linear Correlation
ε	Molar Extinction Coefficient
λ	Wavelength
$\bullet\text{OH}$	Hydroxyl Radical
Fe^{2+}	Iron (II) Ion
H^+	Hydrogen Ion
HO_2^-	Hydroperoxyl Ion
$\text{HO}_2\bullet$	Hydroperoxyl Radical
$\text{O}_2\bullet^-$	Superoxide Radical
OH^-	Hydroxide Ion
$\text{R}\bullet$	Organic Radical
$\text{RO}_2\bullet$	Organic Peroxide Radical
$\text{ROO}\bullet$	Organic Peroxyl Radical
$\text{SO}_4\bullet^-$	Sulphate Radical
Ag	Silver
Al_2Cl_3	Aluminium Chloride
Alum	Aluminium Sulphate
CO_2	Carbon Dioxide
FeCl_3	Ferric Chloride
FeSO_4	Ferrous Sulphate
H_2O	Water
H_2O_2	Hydrogen Peroxide
KMnO_4	Potassium Permanganate
$\text{Na}_2\text{C}_2\text{O}_4$	Sodium Oxalate
Na_2CO_3	Sodium Carbonate
NaOCl	Sodium Hypochlorite
$\text{NH}_3\text{-N}$	Ammoniacal Nitrogen
O_2	Oxygen
O_3	Ozone
TiO_2	Titanium Dioxide

AOPs	Advanced Oxidation Processes
AOTs	Advanced Oxidation Technologies
BOD	Biochemical Oxygen Demand
CF	Coagulation-Flocculation
COD	Chemical Oxygen Demand
DOE	Department of Environment
EFB	Empty Fruit Bunches
FFB	Fresh Fruit Bunches
FP	Primary Quantum Yield
FT	Total Quantum Yield
HRT	Hydraulic Retention Time
MTBE	Methyl tert-Butyl Ether
O&G	Oil and Grease
ODE	Ordinary Differential Equation
PFS	Palm Kernel Shell
POME	Palm Oil Mill Effluent
PPF	Palm Press Fibre
SCE	Saturated Calomel Electrode
SS	Suspended Solid
T&O	Taste and Odour
Temp	Temperature
TKN	Total Kjeldahl Nitrogen
TN	Total Nitrogen
TNB	Tenaga National Berhad
TOC	Total Organic Carbon
TOrC	Trace Organic Chemical
TS	Total Solid
TSS	Total Suspended Solid
TVS	Total Volatile Solid
UV	Ultraviolet
UV-Vis	Ultraviolet-Visible Spectroscopy
VFA	Volatile Fatty Acid
VUV	Vacuum Ultraviolet

CHAPTER 1

INTRODUCTION

1.1 Utilizing Advanced Oxidation Process for Diluted Palm Oil Mill Effluent Treatment

Malaysia is now the second-largest manufacturing and exporting nation of palm oil in the world due to the popularity of palm oil. Today, Malaysia produces 25.8% and exports 34.3% of the world's palm oil. According to Parveez (2023), Malaysia has 450 palm oil mills, processing 119.36 million tonnes of fresh fruit bunches (FFB) annually as of 2022. Of the total number of mills, slightly more than half were situated in Peninsular Malaysia, possessing a combined processing capability of 59.63 million tons. The states of Sabah and Sarawak accounted for 28.4% and 18.7% of the aggregate processing capacity, handling 34.31 million tonnes and 25.42 million tonnes, respectively. Due to a larger quantity of fresh fruit bunches being processed in 2022 compared to 2021, the overall milling capacity utilization rate improved by 0.70%, rising from 77.56% to 78.13%. There were 52 operational palm oil refineries in the refining sector during 2022. These refineries processed 26.90 million tonnes of crude palm oil and kernel oil. While 12 refineries in Sabah and 6 in Sarawak had processing capabilities up to 8.73 million tonnes and 3.12 million tonnes, respectively, the 34 refineries in Peninsular Malaysia possessed a processing capacity of 15.05 million tonnes. Malaysia's complete refining capacity utilization rate exhibited a marginal increase from 56.85% in 2021 to 57.78% in 2023, signifying a growth of 1.60% to meet the escalating demand for processed palm oil in export markets.

In Malaysia, the palm oil industry has contributed significantly to the country's economic development and expansion. However, the extraction operations have resulted in severe environmental damage due to the production of various by-products. There are three main waste streams generated during palm oil processing:

- Solid wastes consist of empty fruit bunches (EFB), palm press fibre (PPF), trash, and palm kernel shell (PFS).
- Liquid wastes comprised of palm oil mill effluent (POME).
- Some gaseous emissions in mechanized farms.

When manufacturing one tonne of crude palm oil, approximately 5–5.7 tonnes of water is required, with 50% converted into POME during the sterilization process of the palm fruit bunches and clarification of extracted oil (Kamyab et al., 2018). In Malaysia, the palm oil sector has the potential to produce 50 to 65 million tonnes of POME yearly (Julia, Munoz-Erazo, and Kemp, 2020). Palm Oil Mill Effluent (POME) possesses exceptionally high biochemical and chemical oxygen demand (BOD and COD). When released from mills, it poses severe environmental risks by potentially contaminating surrounding waterways, rivers, or land. Spilling into bodies of water creates an unpleasant, slimy, and brown appearance. It jeopardizes aquatic species by depleting oxygen levels and hinders humans from accessing clean water for domestic purposes (Iwuagwu and Ugwuanyi, 2014). Therefore, to minimize its detrimental effects on the environment, effective treatment and management of POME are crucial before its discharge into water bodies.

In the 1980s, researchers initially proposed advanced oxidation processes (AOPs) for potable water treatment. These methods aim to oxidize organic and inorganic pollutants in water and wastewater through reactions involving hydroxyl radicals ($\bullet\text{OH}$) (AWC, n.d.). Extensive research has since been conducted on AOPs for various wastewater treatment applications. A range of AOPs exists, including radiation, photolysis and photocatalysis, sonolysis, electrochemical oxidation technologies, Fenton-based reactions, and ozone-based processes. Reactive free radical generation is crucial for the functioning of AOPs, with the hydroxyl radical ($\bullet\text{OH}$) being particularly significant (Wang and Xu, 2012). In water and wastewater treatment, the hydroxyl radical is the most reactive oxidizing agent due to its high oxidation potential that spans from 2.8 V (pH 0) to 1.95 V (pH 14) against SCE, the

commonly used reference electrode. When reacting with various species, $\bullet\text{OH}$ demonstrates a relatively nonselective behaviour. Due to its short life-span, hydroxyl radicals can only be generated in situ using techniques like a mixture of oxidizing agents (e.g., H_2O_2 and O_3), irradiation (e.g., ultrasound or UV light), and catalysts (e.g., Fe^{2+}) (Deng and Zhao, 2015). AOPs, however, offer the advantage of possibly bringing down concentrations of pollutants from several hundred parts per million (ppm) to less than five parts per billion (ppb), which would also dramatically lower levels of total organic carbon (TOC) and chemical oxygen demand (COD) (Munter, 2001). The use of AOP technology in wastewater treatment has been proven effective over time; however, further research is still being conducted for optimal optimization.

1.2 Problem Statements

POME, which refers to palm oil mill effluent, is highly contaminated compared to municipal sewage. It exhibits high biochemical oxygen demand (BOD) and chemical oxygen demand (COD) levels. Moreover, POME contains significantly higher concentrations of organic nitrogen, phosphorus, and other supplement substances. Managing POME poses excellent difficulty due to its large production volume at once and the costly treatment required. Consequently, many palm oil mills in Malaysia opt for the simplest and least expensive method: releasing treated POME into neighbouring rivers or streams (Osman et al., 2020). Unfortunately, this improper management leads to widespread contamination of waterways and poses risks to communities depending on them for drinking water, recreation activities, and fishing opportunities. In recent decades, the unfavourable discharge of POME has emerged as a significant concern for both the environment and public health. The mismanagement of POME has intensified in recent years, prompting the Department of Environment (DOE) to strengthen regulations regarding its discharge. Palm oil mills are now required to reduce POME's biochemical oxygen demand (BOD) to below 20 ppm before it can be released into nearby rivers (Loh et al., 2013). However, the final treatment process in the aerobic pond system struggles to meet these discharge standards due to ineffective operational design. Consequently, the treated POME must comply with strict criteria set by the Malaysian Department of Environment (DOE).

Therefore, palm oil mills in Malaysia should consider implementing tertiary treatment methods, such as advanced oxidation processes (AOPs), to address the challenges and ensure a more efficient and sustainable solution for treating diluted POME. One effective AOP technique is UV/H₂O₂, which offers enhanced removal of organic pollutants and improves diluted POME treatment. This technique utilizes hydrogen peroxide (H₂O₂) as a source reagent to generate hydroxyl radicals with exceptional oxidation potential ($E_0 = 2.80 \text{ V}$), surpassing that of hydrogen peroxide itself ($E_0 = 1.80 \text{ V}$) (Elfiana and Fuadi, 2019). In other words, UV/H₂O₂-AOPs utilize UV light to trigger the breakdown of hydrogen peroxide, generating highly reactive hydroxyl radicals (Sun et al., 2023). When exposed to UV light, these hydroxyl

radicals possess enhanced reactivity, facilitating a more rapid and thorough oxidation process for organic compounds in the effluent. Consequently, this approach significantly enhances the degradation efficiency of organic pollutants in POME compared to UV or H₂O₂ alone. Additionally, AOPs can benefit from the UV/H₂O₂ system through its fast reaction rates and adaptable reactor design, ultimately reducing its overall footprint within treatment facilities. Hence, the system's flow rate can be efficiently processed using minimal land due to the powerful oxidizing ability of the OH radical (Krishnan et al., 2017).

Advanced oxidation processes (AOPs) perform excellently in treating refractory wastewater. In addition to not creating secondary pollutants, they provide high oxidation efficiency (Saravanan et al., 2022). Ultimately, AOPs contribute to a cleaner and more environmentally friendly treatment process. According to Del Moro et al. (2013), combined UV and H₂O₂ facilitate the degradation of various organic compounds, including recalcitrant and complex pollutants that might resist traditional treatment approaches. This broad-spectrum efficacy significantly enhances overall treatment efficiency. For the treatment of POME, several research papers have been published, including those on the moving-bed biofilm reactor technology (Abu et al., 2018), nano-composite membrane (Anwar and Arthanareeswaran, 2019), catalysis (Zainuri et al., 2018), and the electro-coagulation-peroxidation approach (Bashir et al., 2019), among others. Treatment for POME has been documented using a variety of techniques. However, no study has reported UV/H₂O₂ treating diluted POME on the pilot or large scale. To the best of our knowledge, peer-reviewed literature does not yet exist that utilizes the data from optimized lab-scale systems to verify pilot-scale investigations. It is the first documented investigation into using upscaling UV/H₂O₂ advanced oxidation processes for diluted POME treatment. Apart from that, no published work addresses the effect of H₂O₂ dosage ways, including one-time dosing or pulse dosing in UV/H₂O₂ systems for the degradation of treated POME. Furthermore, limited information on applying UV/H₂O₂ for •OH radical scavenging in palm oil mill effluents is available.

1.3 Aims and Objectives

This research aims to investigate treatments for diluted palm oil mill effluent (POME) utilizing the UV/H₂O₂ advanced oxidation method. This study aims to achieve the following three main objectives:

- i) To study the treatment of diluted POME using UV/H₂O₂ treatments in both lab scale and upscaling experiments.
- ii) To optimize the H₂O₂ dosage and the number of UV light used during the photodegradation of palm oil mill effluent using UV/H₂O₂.
- iii) To investigate the kinetic order and cost analyses in treating palm oil mill effluent.

1.4 Scope of Study

This study assesses the efficacy of treating diluted palm oil mill effluent (POME) using the UV/H₂O₂-based Advanced Oxidation Process (AOP). Biochemical Oxygen Demand (BOD) testing and Ultraviolet-Visible Spectroscopy (UV-Vis) will be used to precisely measure the treatment efficacy of POME samples collected from a nearby palm oil mill. Different dosage ways of H₂O₂ and the number of UV light will be explored to optimize the treatment of POME. Additionally, the study aims to determine the reaction order, energy efficiency, and electrical cost of UV in the degradation process by conducting kinetic order analysis and evaluating the cost of POME treatment. The phytotoxicity of the treated POME will also be examined in this study by using mung bean seeds to assess the residual toxicity of the solution.

CHAPTER 2

LITERATURE REVIEW

2.1 Review of the Effluent Derived from Palm Oil Industry

While the palm oil industry is a vital contributor to the global production of vegetable oils, its rapid growth has sparked concerns regarding environmental sustainability. A critical issue associated with palm oil manufacturing is the generation of effluent, a by-product that poses severe environmental and social implications. The liquid waste called Palm Oil Mill Effluent (POME) is characterized by its thick, dense, and brownish appearance, high concentration of colloidal particles suspended in it, and an unpleasant odour (Ahmad and Chan, 2009). POME combines condensate from sterilization, sludge residue from separators, and wastewater from hydrocyclones. Its composition comprises 95-96% water, 0.6-0.7% oil, and 4-5% particulate matter, wherein 2-4% of the particles are suspended solids (Mohammed and Chong, 2004; Prasertsan and Prasertsan, 1996). It has a pH of 4-5 and is hot (80–90 °C). The untreated effluent is bound to create severe environmental issues if discharged into water bodies due to its extremely high levels of biochemical oxygen demand (25,000 mg/L), chemical oxygen demand (50,000 mg/L), oil and grease content (4000 mg/L), total solids (40,500 mg/L), and suspended solids (18,000 mg/L) (Ahmad et al., 2003). Table 2.1 illustrates the usual POME characteristics that were obtained from previous research.

Table 2.1: Characteristics of Palm Oil Mill Effluent from Previous Case Studies

Parameter (mg/L)	Latif Ahmad, Ismail, and Bhatia (2003)	Ma and Ong (1985)	Zinatizadeh et al. (2006)	Zainal (2018)	Wu et al. (2007)	Choorit and Wisarnwan (2007)	Zhang et al. (2008)	Oswal et al. (2002)
BOD₃	25 000	25 000	22 700	25 000	-	65 714	-	11 000
COD	50 000	-	44 300	51 000	70 900	102 696	79 723	246 000
TS	40 500	-	-	-	-	72 058	67 200	-
TVS	-	-	-	34 000	-	-	49 300	-
SS	18 000	19 000	19 780	18 000	25 800	46 011	-	-
O&G	4000	8000	4850	4000-6000	-	9341	17 410	-
NH₃-N	-	35	-	35	-	103	72.8	-
TN	750	770	-	750	-	-	-	-
TKN	-	-	780	-	-	1381	672	-
VFA	-	-	2510	-	-	4202	2287	-
pH*	4.7	4.5	4.05	9.0	4.52	4.4	4.8	5
Temp (°C)	-	80-90	-	85	-	-	-	-

* No unit

Notes: TS – Total Solid; TVS – Total Volatile Solid; NH₃-N – Ammoniacal Nitrogen; TN – Total Nitrogen; TKN - Total Kjeldahl Nitrogen; VFA – Volatile Fatty Acid; Temp – Temperature.

Therefore, POME must be treated before it can be discharged since it is acidic and still includes residual oil that is difficult to separate using traditional gravity-based techniques. This oily mixture takes a lot of oxygen to break down entirely. This phenomenon has a high biochemical oxygen demand, and raw POME has a BOD that is up to 100 times greater than home sewage (Lokman et al., 2019). POME burdens the environment since, despite treatment, it still includes a sizable quantity of organic materials. While consuming organic stuff, water-borne microbes absorb dissolved oxygen. The BOD, or biochemical oxygen demand, is often expressed in milligrams per litre (mg/L), and it measures the amount of organic pollution in water and the quality of its organic content. A more incredible BOD indicates worse quality, and vice versa. The microbial population has been discovered to grow in direct proportion to the food available. Under these circumstances, dissolved oxygen in the water will be consumed by microbial activity more quickly than it can dissolve in the air. The lack of oxygen in the water body may cause the death of fish and other aquatic life (Madaki and Seng, 2013).

On top of that, POME can contaminate drinking water for both people and animals when it is discharged into streams. The crude effluent includes suspended particulates, soil particles, residual oil, and 90–95% water. The wastewater a contemporary oil palm plant produces is 2.5 tonnes per tonne of palm oil or 0.5 tonne per tonne of brand-new, fresh fruit (Sohn et al., 2004). Much research has been done on reducing the harm that palm oil plant wastewater poses to the environment and human health. Creating extremely acidic conditions or eutrophication, which results in severe algae growth on the water's surface, frequently endangers the aquatic ecosystem. POME can have an impact on the physio-chemical characteristics of soil as well. While soil pH drops following biodegradation, soil acidity increases when POME is released. The soil's pH impacts a plant's capacity to absorb the correct quantity of nutrients. If the soil has a higher acidity, even nutrients like nitrogen, phosphorus, and potassium do not boost crop output (Meena et al., 2023). So, treating POME before discharging it into the nearby river is an important step that might reduce the likelihood of water contamination.

2.2 Conventional Treatment for POME

Palm oil is one of the most widely used vegetable oils globally, serving as a crucial ingredient in various food, cosmetic, and industrial products. However, the generation of palm oil mill effluent (POME) is one of the most urgent environmental difficulties brought about by the rapid increase of palm oil production. POME, a highly polluting byproduct of milling palm oil, has significant concentrations of hazardous chemicals, suspended particles, and organic materials. If left untreated, it can cause severe environmental degradation and threaten aquatic life and human health. Therefore, POME treatment is a significant issue for palm oil mills, and the treatment method has captured the interest of many academics studying environmental contamination (Yashni et al., 2020). Several conventional treatments of POME include ponding systems, anaerobic digestion, and coagulation-flocculation.

In Malaysian palm oil mills, anaerobic ponding systems account for more than 85% of treatment processes; other mills use open digesting tanks (Bello and Abdul Raman, 2017). A ponding system is used to treat POME, and this configuration is also referred to as waste stabilization ponds of acidic to final polishing ponds, including an overall hydraulic retention time (HRT) of 100–120 days before release to the environment. The acidification pond received a pumping of the raw POME from the oil-trapping pond, which was held there for around six days (Mohammad et al., 2021). After that, a cooling tower poured the POME into a cooling pond, which was kept for seven days. Before the anaerobic stage, the cooling pond stabilized the pH, which lowered the POME temperature to 35–38 °C. The high starting temperature of POME after cooling encourages anaerobic and thermal digestion, primarily by acidogenesis and hydrolysis. Although the ponding system is cost-effective and can support the high organic loading rate, the long hydraulic retention time and large pond area required have become a massive limitation (Zainal et al., 2018). Besides that, this treatment method cannot wholly decolourize the palm oil mill effluent (Tamrin and Zahrim, 2016).

In contrast, the anaerobic system would be superior to the ponding system due to the greater organic conversion efficiency of chemical oxygen demand (COD), biochemical oxygen demand (BOD), total suspended solid (TSS), and colour, followed by oil and grease (O&G) (Chan, Chong, and Law, 2012). According to Saleh et al. (2011), a series of processes, including hydrolysis, acidogenesis (which includes acetogenesis), and methanogenesis, are involved in the breakdown of POME into methane, carbon dioxide, and water. Complex molecules, including proteins, lipids, and carbohydrates, are hydrolyzed to create sugar, amino acids, and other compounds. Acidogenic bacteria break down these sugars, fatty acids, and amino acids into organic acids, most composed of acetic acid (from acetogenesis), hydrogen, and carbon dioxide. While acetoclastic methanogens use acetic acid and carbon dioxide to produce methane as a product, hydrogenotrophic methanogens use hydrogen and carbon dioxide. However, anaerobic systems have been noted to be laborious, even for plants starting for up to 4 months, with varying up-flow velocities as well as generated granules washouts from hydraulic stress (Poh and Chong, 2014). In addition, specific biological treatments need intricate management of variables, including feed flow rate, up-flow velocity, COD, pH, and biomass content. The variables significantly influence the alkalinity and total volatile fatty acids in treated wastewater, which affects the effectiveness of biological treatment (Mohammadi et al., 2017).

Coagulation-flocculation (CF) is another widely used physicochemical method in POME therapy. Large colloidal particle masses can be formed by coagulation. Two distinct processes lead to the accumulation of colloidal particles: (1) Particle movement to create interparticle contact and (2) Particle dislocation to enable attachment as contact progresses (Alhaji et al., 2016). The coagulant/flocculant type affects how well the primary POME parameters are reduced by this approach (Huzir et al., 2019). On the other hand, the kind and quantity of coagulant/flocculant, pH, mixing speed, temperature, and retention time are other variables that impact coagulation and flocculation (Zinatizadeh et al., 2017). For dewatering coagulation and sludge conditioning procedures, hydrated lime, ferrous sulphate (FeSO_4), ferric chloride (FeCl_3), aluminium chloride (Al_2Cl_6), aluminium sulphate (alum), and poly-aluminium chloride are the most often utilised

coagulants. The CF process does have significant downsides, though, since it can create harmful activated sludge, such as acrylamides when treating wastewater that has been chlorinated. For instance, using aluminium sulphate as a coagulant for wastewater treatment has been criticised for producing hazardous activated sludge connected to Alzheimer's disease (Bashir et al., 2017).

The environmental stewardship of the palm oil sector includes the sustainable management of palm oil mill wastewater. Conventional treatments such as ponding systems, anaerobic digestion, aerobic therapy, coagulation-flocculation, and membrane filtration play a significant role in reducing the environmental impact of POME. These treatments not only alleviate pollution but also offer opportunities for resource recovery, such as biogas production and the use of digestate as fertilizer. Under ideal operating conditions, conventional treatment technologies can meet the required BOD effluent discharge limitations of 100 mg/L. Most of the deployed technologies do not regularly achieve 100% compliance with the BOD (20 mg/L) recently suggested by Malaysia's Department of Environment (DOE) due to uncertainty in plant performance (Wang et al., 2015). Table 2.2 shows the current and future standard discharge limits of the final discharge of POME set by DOE. The oil palm sector is required to research a wide range of methods to cure POME in some sensitive areas, particularly those involving tourism activities in Sabah and Sarawak. Therefore, an advanced treatment must be applied as the tertiary treatment of POME to fulfil the requirements set by DOE in Malaysia.

Table 2.2: Standard Discharge Limits of POME Final Discharge Set by DOE

Parameter	Current Standard Discharge Limit (DOE, 1982)	Future Standard Discharge Limit (Zainal, 2018)
BOD ₃ (mg/L)	100	20
COD (mg/L)	*	*
TS (mg/L)	*	*
SS (mg/L)	400	200
O&G (mg/L)	50	5
NH ₃ -N (mg/L)	150	-
TN (mg/L)	200	150
pH	5-9	5-9
Temp (°C)	45	45

* No discharge standard after year 1984.

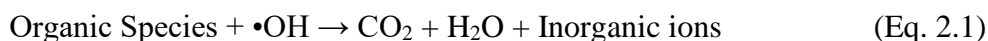
Notes: TS – Total Solid; SS – Suspended Solid;

NH₃-N – Ammoniacal Nitrogen; TN – Total Nitrogen;

Temp – Temperature.

2.3 Advanced Oxidation Processes (AOPs)

Advanced oxidation processes (AOPs), which are defined as oxidation processes including the formation of hydroxyl radicals ($\bullet\text{OH}$) in sufficient quantity to impact water purification, were initially proposed for the treatment of potable water in the 1980s (Deng and Zhao, 2015). AOPs are regarded as very efficient wastewater treatment technology for eliminating contaminants with limited biodegradability, refractoriness, inhibitory effects, or high chemical stability. The AOPs processes depend on the in-situ synthesis of highly reactive oxidant species, primarily hydroxyl radicals ($\bullet\text{OH}$). The $\bullet\text{OH}$ radicals have a 2.8 V redox potential, electrophilic behaviour, and are highly effective, robust, and abundant in nature. They speed up the oxidation and degradation of various contaminants in wastewater by removing a hydrogen atom from aliphatic carbon or adding a hydrogen atom to double bonds and aromatic rings (Wang et al., 2011; Oturan and Aaron, 2014). In extreme cases, the OH molecules can even mineralize them into carbon dioxide (CO_2), water (H_2O), and inorganic salts.



Within the class of potential oxidants, hydroxyl radicals excel because they satisfy several criteria (Cuerda-Correa, Alexandre-Franco, and Fernández-González, 2019):

- They do not produce extra garbage.
- They have a short lifespan and are not poisonous.
- They seldom cause equipment to corrode.
- They are often constructed using easy-to-manipulate structures.

These factors indicate that AOPs are environmentally friendly technologies and competitive economic processes are being created on their foundation. The lifespan of AOPs is determined by the effectiveness of the $\bullet\text{OH}$ radical, the second species after fluorine with a higher oxidant potency (Guinea et al., 2008; Brillas, Sirés, and Oturan, 2009). Table 2.3 shows the standard reduction potentials for several kinds of oxidants.

Table 2.3: Standard Reduction Potential for Different Oxidants (Cuerda-Correa, Alexandre-Franco, and Fernández-González, 2019)

Oxidizer	Standard Reduction Potential (V)
Fluorine	3.05
Hydroxyl radical	2.80
Sulphate radical anion	2.60
Ferrate	2.20
Ozone	2.08
Peroxodisulphate	2.01
Hydrogen peroxide	1.76
Permanganate (1)	1.67
Hydroperoxyl radical (1)	1.65
Permanganate (2)	1.51
Hydroperoxyl radical (2)	1.44
Dichromate	1.36
Chlorine	1.36
Oxygen	1.23

Notes: (1) Circumneutral or mildly acidic medium; (2) Strongly acidic medium

The radicals involved in AOPs contribute to their remarkable efficiency on thermodynamic and kinetic grounds. The hydroxyl radical reacts 10^6 – 10^{12} times faster than other oxidants, such as ozone (O_3), and can attack nearly all organic compounds. $\bullet OH$, is the most energetic oxidant, second only to fluorine, as seen in Table 2.3. Table 2.4 shows that the reaction rates of different compounds with $\bullet OH$ are faster than those with O_3 . But it's important to note that producing plenty of hydroxyl radicals at a constant state is where advanced oxidation technologies (AOTs) get their efficiency. Other active oxygen species generated in various AOTs include the superoxide radical ($O_2^{\bullet -}$) and its conjugate acid form, the hydroperoxyl radical (HO_2^{\bullet}). However, they are significantly less active than $\bullet OH$ (Litter, 2005).

Table 2.4: Rate Constants (k in $M^{-1}s^{-1}$) for Ozone and Hydroxyl Radical Reactions with Different Organic Compounds (Litter, 2005)

Compound	$\bullet\text{OH}$	O_3
Chlorinated Alkenes	$10^9 - 10^{11}$	$10^{-1} - 10^3$
Phenols	$10^9 - 10^{10}$	10^3
Aromatics	$10^8 - 10^{10}$	$1 - 10^2$
Ketones	$10^9 - 10^{10}$	1
Alcohols	$10^8 - 10^9$	$10^{-2} - 1$
Alkanes	$10^6 - 10^9$	10^{-2}

Generally, there are four main methods by which hydroxyl radicals destroy organic pollutants: radical addition, hydrogen abstraction, electron transfer, and radical combination (Deng and Zhao, 2015). Radicals ($R\bullet$ or $R\bullet\text{OH}$) with a carbon nucleus are the products of their reactions with organic molecules. These carbon-centre radicals can become organic peroxy radicals ($\text{ROO}\bullet$) in the presence of oxygen. All the radicals continue to react, producing highly reactive species such as superoxide ($\text{O}_2\bullet^-$) and hydrogen peroxide (H_2O_2), which causes the chemical breakdown and even mineralization of these organic molecules. The hydroxyl radical may also remove an electron from electron-rich substrates to create a radical cation, which is readily hydrolyzed in aqueous conditions and eventually results in an oxidized product. The oxidation products are frequently less toxic and more amenable to bioremediation (O'Shea and Dionysiou, 2012). Due to their short half-lives, $\bullet\text{OH}$ can only be created in situ during application by a variety of methods, including the combination of oxidizing agents (such as H_2O_2 and O_3), irradiation (such as ultrasound or UV light), and catalysts (such as Fe^{2+}) (Huang, Dong, and Tang, 1993). Adding an oxidant or altering the irradiation settings allows the water treatment plant to transition from the regular UV disinfection mode to disinfection and taste and odour (T&O) control if T&O compounds are present (Zoschke et al., 2012). Therefore, the present study focuses on applying UV-based AOPs, specifically in UV/ H_2O_2 , to meet the criteria of discharge standard of POME, which is 20 mg/L of BOD.

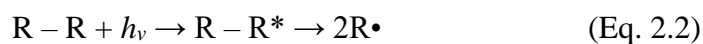
2.4 UV Based of AOPs

The UV advanced oxidation process (UV/AOP) is a multipurpose advanced treatment technique frequently used in water and wastewater treatment systems to inactivate microorganisms and photolyze and oxidize target contaminants simultaneously (Vinge et al., 2021). They offer the advantage of being able to degrade complex pollutants effectively without producing harmful by-products. When choosing the appropriate AOP for a particular application, it's essential to consider the specific pollutants present, the required treatment efficiency, and the cost-effectiveness. There are several types of UV-AOPs, including UV direct photolysis, heterogeneous photocatalysis, UV/H₂O₂, and UV/O₃ processes. Table 2.5 shows the principal methods for organics removal during wastewater treatment by various AOPs.

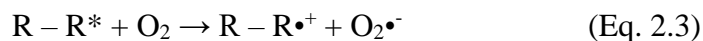
Table 2.5: Major Methods for Organics Removal during Wastewater Treatment by Various AOPs (Deng and Zhao, 2015)

AOP Types	Oxidant for AOP	Other Occurring Mechanisms
O ₃	•OH	Direct O ₃ Oxidation
O ₃ /H ₂ O ₂	•OH	Direct O ₃ Oxidation H ₂ O ₂ Oxidation
O ₃ /UV	•OH	UV Photolysis
UV/TiO ₂	•OH	UV Photolysis
UV/H ₂ O ₂	•OH	UV Photolysis H ₂ O ₂ Oxidation
Fenton reaction	•OH	Iron Coagulation Iron Sludge-Induced Adsorption
Photo-Fenton reaction	•OH	Iron Coagulation Iron Sludge-Induced Adsorption UV Photolysis
Heat/persulphate	SO ₄ • ⁻	Persulphate Oxidation UV Photolysis

First and foremost, the breakdown process that emerges from the absorption of incoming energy from the UV light serves as the primary elimination mechanism in UV direct photolysis. Consequently, the application typically focuses on contaminants significantly absorbing UV rays. Deng and Zhao (2015) state that most UV light absorbers present delocalized electrons and double or conjugated double bonds made of carbon, nitrogen, or oxygen atoms. A photon of 254 nm, for example, has an energy of 4.89 eV, which is enough to shatter molecules either homolytic or heterolytically. A molecule can be excited from its ground state to a higher energy singlet state by absorbing light radiation directly. This singlet excited state can undergo intersystem crossing to form a triplet excited state. These excited singlet and triplet states can further dissociate or ionize through mechanisms like homolysis (forming radicals), heterolysis (forming ions), or photoionization. Most frequently, homolytic rupture results in radicals:



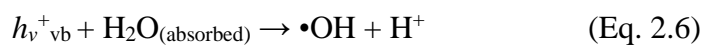
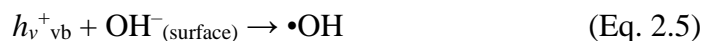
These radicals trigger a chain reaction that results in the final low-weight compounds. The superoxide radical may break down substituted aromatic compounds that absorb much of UV light despite having a relatively low oxidising power (Litter, 2005). Additional processes that can produce the superoxide radical in the presence of oxygen include:



For heterogeneous photocatalysis, hydroxyl radicals are initiated by photons in the presence of a catalyst. Titanium dioxide (TiO₂), a RO-type semiconductor, is the most used catalyst. TiO₂ particles are energised to form positive holes in the valence band ($h\nu^+_{vb}$) with an oxidative capacity and negative electrons at the conduction band (e^-_{cb}) with a reductive capacity as follows:



These holes and electrons can further combine to create hydroxyl radicals through the interactions of OH^- , H_2O , and $\text{O}_2^{\bullet-}$ at the surface of TiO_2 (Deng and Zhao, 2015).



In the UV/ O_3 process, dissolved ozone is split apart by UV light ($\lambda < 300$ nm), followed by a quick reaction between atomic oxygen and water to create thermally excited H_2O_2 . The excited peroxide breaks into two $\bullet\text{OH}$ (von Sonntag, 2008). At $\lambda = 254$ nm, the molar extinction coefficient of ozone is $\varepsilon = 3300 \text{ M}^{-1}\text{cm}^{-1}$, which is much greater than that of H_2O_2 at this specific wavelength. However, only a tiny percentage of the produced H_2O_2 decomposes to $\bullet\text{OH}$ due to cage recombination, resulting in a free $\bullet\text{OH}$ quantum yield of only 0.1 (Reisz et al., 2003). UV and ozone have very significant energy requirements due to the enormous electrical energy requirements of both UV lamps and ozone generators. The key benefit of this technique is that it can directly oxidise a broad spectrum of trace organic chemicals (TOxC) reactivity using ozonation and photolysis (Miklos et al., 2018).

The UV/ H_2O_2 advanced oxidation process (AOP) is a water treatment method that uses UV light and an oxidant, such as hydrogen peroxide or chlorine, to produce hydroxyl radicals that can break down organic and inorganic contaminants. The photolytic cleavage of H_2O_2 into two $\bullet\text{OH}$ is caused by the interaction of UV light with H_2O_2 (Miklos et al., 2018). According to Morgan et al. (1988), the molar absorption coefficient of H_2O_2 at 254 nm was $18.6 \text{ M}^{-1}\text{cm}^{-1}$ and the quantum yield of $\bullet\text{OH}$ generation was 0.5-1.1 mol E^{-1} . $\bullet\text{OH}$ may quickly and non-selectively destroy contaminants due to its high redox potential ($E_0 = 2.8 \text{ V}$) (Li et al., 2017). The UV/ H_2O_2 treatment method proved efficient in oxidising POME under ideal circumstances (Affam and Bin Bistar, 2020). Although hydrogen peroxide alone is not as efficient as UV-mediated AOP employing chlorine and the active chlorine species, UV/ H_2O_2 AOP has also been successful at disinfecting water (Xiang et al., 2020). Overall, the POME and other types of water with a high organic matter content may be treated using the UV/ H_2O_2 AOP as a promising technique.

2.5 Mechanisms of Pollutant Degradation in UV/H₂O₂

The UV/H₂O₂ system operates through several mechanisms when oxygen is present, as shown in Figure 2.1 (Legrini, Oliveros, and Braun, 1993). UV/H₂O₂ is also known as UV-peroxidation. It is a chemical oxidation process that uses hydrogen peroxide as a reagent to transform radical hydroxide ($\bullet\text{OH}$) from an excited state (Elfiana and Fuadi, 2019). Using UV/H₂O₂ in water and wastewater treatments has several advantages, the main one being that UV light can work as a disinfectant by physically hindering bacteria and helping to photolyze peroxide, transforming it into a highly reactive $\bullet\text{OH}$ species (Mierzwa, Rodrigues, and Carlos, 2018). The mechanism of the UV/H₂O₂ process can be classified into three phases: initiation, propagation, and termination.

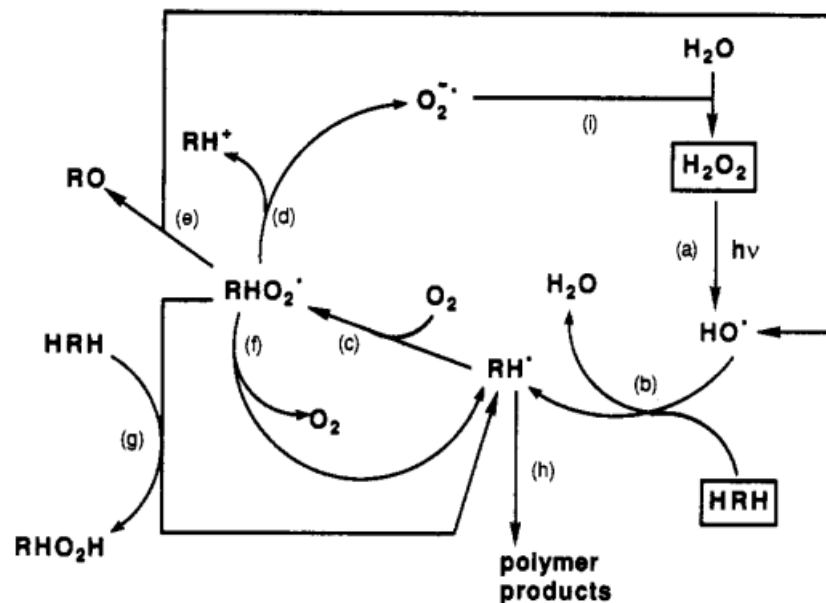
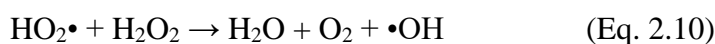
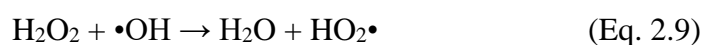


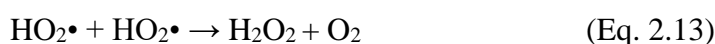
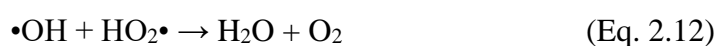
Figure 2.1: Reaction mechanisms for UV/H₂O₂ system (Legrini, Oliveros, and Braun, 1993)

During the initiation phase, the photocatalytic breakdown of H_2O_2 results in two hydroxyl radicals ($\bullet\text{OH}$) forming. In other words, the hydrogen peroxide will ionize to form hydrogen peroxide and hydrogen ions. Direct photolysis of hydrogen peroxide with UV light will form two hydroxyl radicals. According to Crittenden et al. (1999), at the UV light wavelength of 254 nm, the total quantum yield (FT) of hydrogen peroxide in this reaction chain is unity. Still, the primary quantum yield (FP) of the immediate photolysis process of hydrogen peroxide (Equation 2.8) at the same wavelength is 0.5.

The homolytic cleavage of the O-O bond produces hydroxyl radicals, which set off a series of reactions that are described by an initiation step (Equation 2.8), a propagation step provided by reactions (Equation 2.9) and (Equation 2.10), and which are responsible for the photoinduced breakdown of hydrogen peroxide in pure water (Mierzwa, Rodrigues, and Carlos, 2018). In the propagation phase, the hydroxyl radical will react with excess hydrogen peroxide in the water to produce perhydroxyl radical and water. The perhydroxyl radical reacts with hydrogen peroxide to produce one water molecule, oxygen radical and hydroxyl radical.

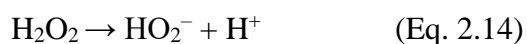


Notably, the breakdown of H_2O_2 into water and molecular oxygen is represented by the net reaction of reactions (Equation 2.9) and (Equation 2.10). During the termination phase, the interaction between two hydroxyl radicals leads to recombination to form hydrogen peroxide. The hydroxyl ion reacts with perhydroxyl radical to produce one hydrogen peroxide and one oxygen. The specific termination processes (Equations 2.11 – 2.13) include radical–radical recombination, as shown below:



The equations 2.9 to 2.13 reveal that while hydrogen peroxide breaks down to generate hydroxyl radicals (Equation 2.8), having too much hydrogen peroxide present can consume the hydroxyl radicals, decreasing the oxidation process's efficiency. Therefore, the initial hydrogen peroxide concentration must be carefully controlled to optimize the removal process. Additionally, hydrogen peroxide is expensive, increasing overall operating costs (Cédât et al., 2016). The highly reactive hydroxyl radicals react with organic compounds in various ways, like inserting into double bonds, removing hydrogen atoms, or transferring electrons, depending on the molecule's structure and functional groups. The most common reaction is hydrogen abstraction, creating an organic radical $R\cdot$ that rapidly reacts with dissolved oxygen to form the organic peroxide radical $RO_2\cdot$ (Legrini, Oliveros, & Braun, 1993). When these organic radicals break down through bimolecular processes, they produce various byproducts from the original molecule and formaldehyde, hydrogen peroxide, and hydroperoxide radicals.

Finally, dimerization of the hydroxyl radicals themselves, the reverse of equation 2.8, and hydroperoxide radicals (equation 2.13) reactions that can then consume hydroxyl radicals (equation 2.9) are responsible for regenerating hydrogen peroxide. It is also necessary to consider the dissociation equilibria of the organic component as well as those of the many intermediates produced, including hydrogen peroxide and hydroperoxide radicals, as illustrated below:

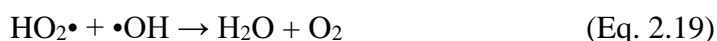
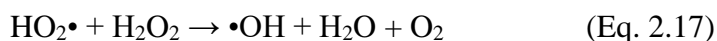
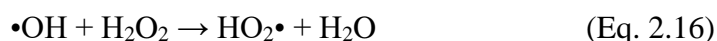


In conclusion, a hydrogen peroxide generation and degradation cycle may be formed. Such a cycle result depends upon several variables, including UV light intensity, pH, temperature, and the type of organic molecules present (Cuerda-Correa, Alexandre-Franco, and Fernández-González, 2019).

2.6 Effect of Operating Parameters

2.6.1 Concentration of H₂O₂

In advanced oxidation processes (AOPs), H₂O₂ is frequently used to treat wastewater. By encouraging the production of hydroxyl radicals (•OH), adding H₂O₂ seeks to improve oxidation and remove chemical components of POME (Parthasarathy, Gomes, and Manickam, 2015). The dominant species responsible for non-selective attack on organic compounds is the •OH radical. The effectiveness of UV/H₂O₂ induced degradation reactions has shown a strong correlation with the concentration of H₂O₂ (Lopez et al., 2000; López Cisneros, Gutarra Espinoza, and Litter, 2002). However, excessively high levels of •OH caused by an excessive introduction of H₂O₂ may result in inefficient reactions and reduced process performance (Tokumura et al., 2011). At high concentrations, competitive reactions occur due to rapid recombination and subsequent generation of H₂O₂.



In Equations 2.16 and 2.19, the consumption of •OH reduces the likelihood of oxidation. Although HO₂• radicals are produced in reaction 1, they are far less reactive than •OH. Using H₂O₂ is necessary, but exceeding the optimal amount can have adverse effects (Yu et al., 2020). Hydrogen peroxide supply is a critical factor in advanced oxidation processes (AOPs) as it influences both reaction outcomes and process costs by regulating the concentration of hydroxyl radicals. Determining the most suitable H₂O₂ concentration depends on the concentration and composition of contaminants in the effluent stream, ensuring that excess H₂O₂ does not impede degradation. Consequently, treatability tests are essential for establishing the ideal H₂O₂ concentration and verifying its efficacy (Litter et al., 2005).

According to Zang and Farnood (2005), it is imperative to get the most out of the UV/H₂O₂ process while keeping costs as low as possible when treating high concentrations of hydrogen peroxide. The reaction rate slows as concentrations rise because HO₂• is less reactive than •OH. It has been found that continuously dosing H₂O₂ can improve oxidation efficiency compared to giving the entire dose during the initial reaction. Studies carried out by Monteagudo et al. (2009) and Zazo et al. (2009) support this finding. Adding discrete quantities of H₂O₂ at various intervals and dividing the whole supply into numerous sections has yielded benefits despite the lack of dosage. However, random periods of addition prevent the solutions from being considered optimal. Several researchers have found that the stepwise addition of H₂O₂ in discrete doses yields better benefits than a single large initial dosage (Chu et al., 2007; Almeida et al., 2015). As suggested by earlier studies, the process efficiency can be boosted by increasing the pace at which H₂O₂ is added to the reactor during the reaction (Monteagudo et al., 2009; Prato-García and Buitrón, 2012). Table 2.6 compares the removal efficiency of one-shot and pulse dosing of different oxidants to treat the specified pollutants.

Table 2.6: Comparison of The Removal Efficiency of One-Time Dosing versus Pulse Dosing for Various Oxidants

Oxidants	Targeted Pollutants	Concentration of Pollutants	Removal Efficiency (%)		Treatment Time Interval for Pulse Dosing (min)	References
			One-Time Dosing	Pulse Dosing		
H ₂ O ₂	Commercial Pesticides	200 mg/L of COD	50	56	10	Prieto-Rodríguez et al. (2011)
H ₂ O ₂	Paracetamol	63 mg/L of TOC	63	75	1	Yu et al. (2021)
H ₂ O ₂ and FeSO ₄	Palm Oil Mill Effluent (POME)	190 mg/L of TOC	66	72	5	Gamaralalage, Sawai and Nunoura (2020)
H ₂ O ₂	Dye Wastewater	20 mg/L	75	95	1	Monteagudo et al. (2009)
H ₂ O ₂	Phenol	100 mg/L	14	18	1	Zazo et al. (2009)
H ₂ O ₂	Indanthrene Blue Dye	60 mg/L	96	99	20	Almeida et al. (2015)
H ₂ O ₂	Atrazine	0.01 mM	14	24	1.5 – 2.5	Chu et al. (2007)

2.6.2 UV Light and Its Intensity

UV-visible light irradiation is necessary to initiate photochemical reactions in molecules. The visible spectrum covers wavelengths from 400-800 nm, while the UV spectrum is divided into UV-A, UV-B, UV-C (shortwave), and VUV (vacuum UV) ranges, as shown in Table 2.7. Sunlight can provide some UV irradiation, though only 3-5% of the solar spectrum is UV light (Litter, 2005). Light often accelerates the reaction rates of advanced oxidation processes (AOPs) compared to dark conditions. Typical light sources are high-pressure mercury or xenon arc lamps emitting near-UV light. Some applications require shortwave UV from inexpensive germicidal lamps. However, light-driven homogeneous AOPs become inefficient for treating highly light-absorbing mixtures or those with suspended particles, as light is lost due to absorption, scattering, and competing for photon absorption. A molecule can be excited from its ground state to a higher energy singlet state by absorbing light radiation directly. This singlet excited state can undergo intersystem crossing to form a triplet excited state. These excited singlet and triplet states can further dissociate or ionize through mechanisms like homolysis (forming radicals), heterolysis (forming ions), or photoionization.

Table 2.7: Various Types of UV Light and Their Applications in Photochemical AOTs (Litter, 2005)

Type	λ (nm)	Energy (kJ mol ⁻¹)	Uses
UV-A*	315 – 400 (365) **	380 – 299 327	Almost all photochemical AOTs
UV-B	280 – 315	427 – 380	Some AOTs
UV-C*	190 – 280 (254, 185)	629 – 427 (471, 646)	Disinfection and sterilization, H ₂ O ₂
VUV*	< 190 (172) **	> 629 695	Some applications

* Used in environmental applications

** The most used wavelength

Light intensity is one of several parameters influencing how quickly organic molecules degrade in photocatalytic processes. Advanced oxidation processes (AOPs) like UV/H₂O₂ systems require UV radiation to produce hydroxyl radicals. These highly reactive radicals can rapidly degrade organic compounds (Andrades et al., 2022). The energy available for forming these radicals depends on how intense the UV light is. More significant amounts of photons from UV light with a higher intensity can activate hydrogen peroxide (H₂O₂) and start the creation of hydroxyl radicals (Zang and Farnood, 2005). After reacting with the pollutants, these hydroxyl radicals transform them into less dangerous and simpler molecules. Higher production of hydroxyl radicals leads to more efficient oxidation of contaminants, which is why the degradation rate speeds up as UV light intensity rises (Hu et al., 2008).

Using the methyl tert-butyl ether (MTBE) pollutant, Hu et al. (2008) observed that increasing the intensity of UV light led to a higher rate of Ag/TiO₂ catalyst degradation of MTBE. Figure 2.2 illustrates the findings about the impact of UV wavelengths on the effectiveness of MTBE removal using typical UV/H₂O₂ system data. The UV light contains more energy at a shorter wavelength (254 nm), which is required to form •OH and other activated substances. Besides that, the study on the degradation of reactive yellow dye showed that the more UV lamps, the higher the intensity, and it subsequently provides more energy to produce hydroxyl radicals (Mohammed, Alward, and S. Salman, 2020). Table 2.8 compares the removal efficiency for different numbers of UV lamps and their intensity.

Table 2.8: Comparison of The Removal Efficiency for Different Numbers of UV Lamps and Their Intensities

Types of UV Light	Intensity (mW/cm ²)	Catalyst	Targeted Pollutants	Concentration of Pollutants	Treatment Time (mins)	Removal Efficiency for Different Number of UV Lamps* (%)				References
						1	2	3	4	
						UV-C	400	TiO ₂	Reactive Yellow Dye	
UV-C	-	Ferrite photocatalyst	Methylene Blue Dye	10 mg/L	60	-	80	-	95	Gupta et al. (2020)
UV-C	-	TiO ₂	Coffee Processing Wastewater	-	180	28	45	55	63	Sujatha, Shanthakumar, and Chiampo (2020)
UV-A	-	-	Nitrobenzene	20 mg/L	60	-	22	-	26	Pérez-Sicairos et al. (2016)
UV-C	-	-	Nitrobenzene	20 mg/L	60	-	88	-	89	Pérez-Sicairos et al. (2016)

*Round off value

2.7 Kinetic Model of UV/H₂O₂ System

According to Pham Minh et al. (2018), kinetic studies are carried out to identify the best-fit reaction rate model that is essentially generated from mechanistic reaction pathways. That best describes the experimental reactant reaction rate and the product creation rate. Kinetic modelling of advanced oxidation processes is a helpful tool for analysing process variables, system optimization, and identifying the ideal parameters for process design. Mathematical modelling of AOPs can be done at multiple levels, depending on the kinetic pathways, reaction rate constants, model pollutant structure, catalyst type, UV light presence, computer resources, and modelling goals (Crittenden et al. 1999; Kusic et al. 2009).

Primo et al. (2007) and Yao et al. (2013) found that the set of ordinary differential equations (ODE) defining the pollutant degradation rate under investigation can be used to create a pseudo-first-order kinetic expression with an exponential solution. Experimental data are fitted to that solution in these kinds of models. As a result, model predictions and lab data agree well. In this research, a first-order kinetic study is commonly carried out to assess the effectiveness of UV/H₂O₂ treatment by one-time dosing and pulse dosing of H₂O₂ on POME's BOD reduction. The pseudo-first-order equation (Equation 2.20) was applied to the data obtained from the experiment. The model explained the relationship between BOD reduction and different dosing methods. The POME initial BOD, BOD of POME at time t, and the pseudo-first-order rate constant of POME reduction are expressed by the variables C₀, C_t, and K, respectively.

$$\ln\left(\frac{C_0}{C_t}\right) = Kt \quad (\text{Eq. 2.20})$$

2.8 Summary of Literature Review

In summary, the first stage of the literature review involved a comprehensive analysis of the features of wastewater from palm oil mill effluents (POME) and a range of traditional treatment techniques employed to degrade POME. Different traditional treatment methods and their limitations in achieving compliance with Malaysia's Department of Environment (DOE) standards, particularly in terms of BOD levels, have been discussed in this section. Advanced oxidation processes (AOPs) like UV-based AOPs were recommended to meet these standards. Among them, the UV/H₂O₂ system was highlighted as a promising technology to overcome the limitations of conventional treatments. To better comprehend the UV/H₂O₂ process, the theory, mechanisms, critical process parameters, and first-order kinetic study of the UV/H₂O₂ system for efficient pollutant degradation in POME were thoroughly examined. Notably, this study intends to explore upscaling UV/H₂O₂ processes from lab-scale to pilot-scale for treating diluted POME, which is a novel aspect. Additionally, it addresses the impact of different H₂O₂ dosage methods and the use of UV/H₂O₂ for scavenging •OH radicals in palm oil mill effluents, areas with limited prior research.

CHAPTER 3

METHODOLOGY

This chapter outlines the materials, equipment, and procedures for examining how UV/H₂O₂ treatment degrades palm oil mill effluent. It evaluates the results regarding colour removal, BOD reduction, and phytotoxicity. It also explored key parameters like UV irradiance and H₂O₂ dosing methods in both laboratory-scale and upscaled experiments. Radical scavenger tests were conducted to understand the active species involved in the degradation process.

3.1 Flowchart of Research Methodology

The progression of this study is summarized in the flowchart shown in Figure 3.1.

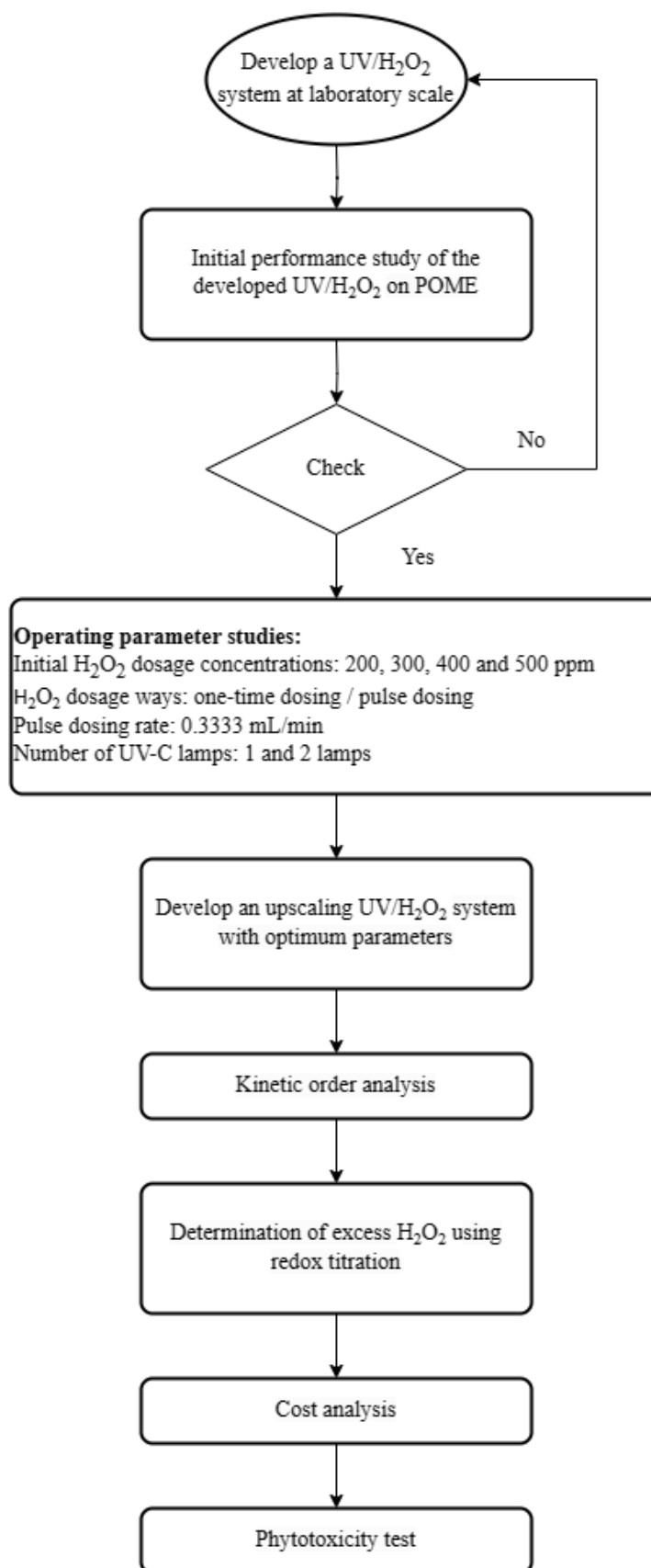


Figure 3.1: Flowchart of Overall Experimental Work

3.2 Chemicals and Materials

Table 3.1 shows the chemicals and materials used in the UV/H₂O₂ advanced oxidation processes (AOPs) to degrade palm oil mill effluents (POME). Every chemical used in the studies was analytical grade, utilized directly from the store without additional purification.

Table 3.1: Inventory of Chemicals and Materials

Chemicals/ Materials		Purity (%)	Source/ Supplier	Application
Distilled (10M Ω ·cm)	Water	N/A	Gainson Advanced Technology	To prepare diluted POME solution
Hydrogen Peroxide (H ₂ O ₂)		50	Spectrum	To conduct H ₂ O ₂ dosage ways study
UV-C Lamp (254 nm)		N/A	Tian Siang Oil Mill Sdn Bhd.	To conduct UV irradiance study
BOD Nutrient Baffle		N/A	HACH Malaysia	To conduct BOD Test
Potassium (KMnO ₄)	Permanganate	99	GENE Chemicals	To determine the excess H ₂ O ₂ in treated POME solution
Sodium (Na ₂ C ₂ O ₄)	Oxalate	99	R&M Chemicals	To determine the excess H ₂ O ₂ in treated POME solution
Sulphuric Acid (H ₂ SO ₄)		96-99	GENE Chemicals	To determine the excess H ₂ O ₂ in treated POME solution
Sodium (NaOCl)	Hypochlorite	0.05	GENE Chemicals	To prepare mug beans for phytotoxicity test
Real Industrial Wastewater	POME	-	Tian Siang Oil Mill Sdn Bhd.	To assess the UV/H ₂ O ₂ system's performance in treating diluted POME

3.3 Experimental Setup

The UV/H₂O₂ treatments for palm oil mill effluent (POME) degradation were carried out in a batch reaction system with a UVP Pen-Ray Mercury Lamp (UV-C lamp, 254 nm). Initially, the jacketed reactor was loaded with 600 mL of 100 ppm POME (Luna, Nascimento, and Chiavone-Filho, 2006). A hot plate stirrer was used to mix the POME solution. A cooling water system was used to control the system temperature as the UV lamps emit a lot of heat, incredibly UV-C light. The cooling water system was set up by the jacketed reactor's cooling water intake, which was linked to the water faucet, and its water output was connected to the basin so that water could circulate and add additional cooling for the system while the experiment was running. The top of the jacketed reactor was used to install the UV lamps with quartz tubes. Before the experiment began, the lamp was turned on for 10 minutes to stabilize the lamp's light output (Andrades et al., 2022). The laboratory-scale experiment was conducted in an acrylic black box to prevent any light from entering. Figure 3.2 illustrates the schematic diagram of a complete UV/H₂O₂ system. The experimental setup at the laboratory scale is depicted in Figure 3.3.

Acrylic black box

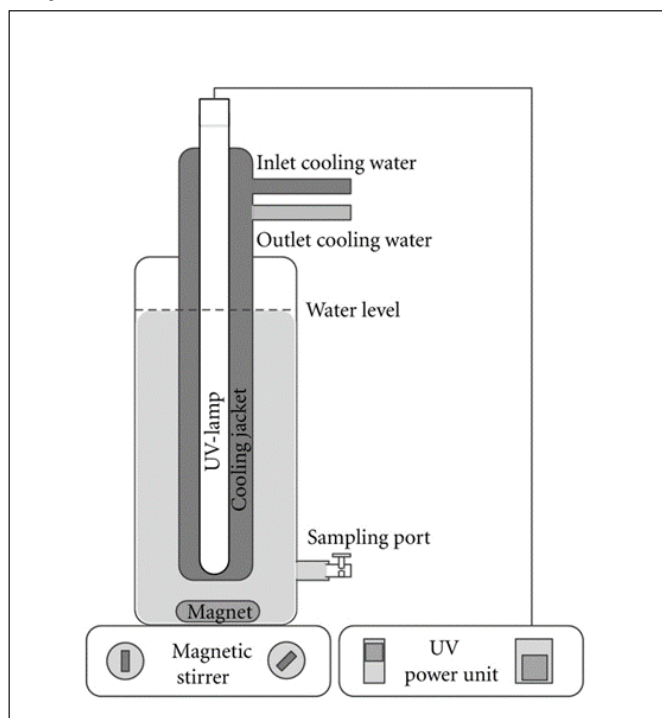


Figure 3.2: Schematic Diagram of UV/H₂O₂ System

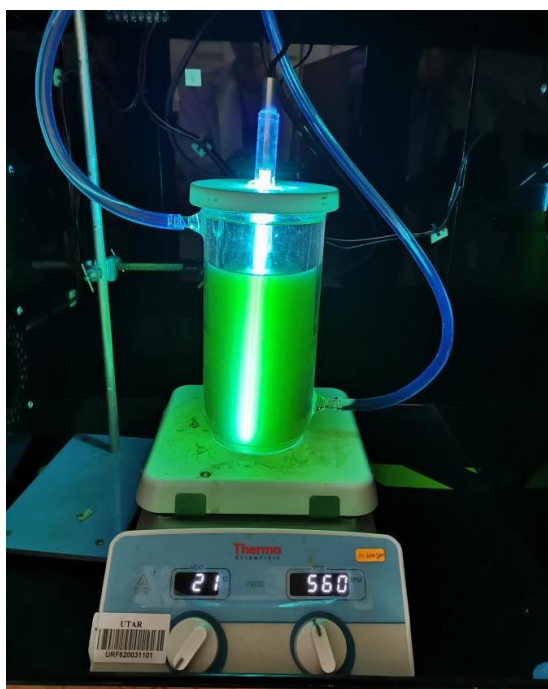


Figure 3.3: Experimental Setup of UV/H₂O₂ System at Laboratory Scale

3.4 Colour and BOD Test

In a typical experiment, the POME was diluted with distilled water up to 600mL for laboratory-scale experiments to create a 100 ppm POME solution. The UV lamp used at the laboratory scale had a measured light intensity of 5.4 mW/cm² for 254 nm. Different concentrations of a 50% H₂O₂ solution were employed to evaluate the impact of H₂O₂ concentration on the degradation process, which are 200, 300, 400, and 500 ppm of H₂O₂ solution, respectively. To measure POME's initial concentration (C_0), a representative sample of diluted POME was taken before H₂O₂ was added. At the beginning of the experiment, the UV-C lamp was turned on for 10 minutes to stabilize the lamp's output. After adding the H₂O₂ in one shot, the solution was periodically sampled (15 mL) at intervals of 30 minutes to measure the POME concentration (C_t). Six hours were spent conducting the entire experiment. A JASCO V-730 UV-vis spectrophotometer was used to measure the concentration of the samples two hours later. The concentration of the samples was next recorded and computed to determine the effectiveness of colour removal. The following formula was used to determine the colour removal efficiency:

$$\text{Colour removal efficiency (\%)} = \frac{C_0 - C_t}{C_0} \times 100\% \quad (\text{Eq. 3.1})$$

C_0 = Initial Concentration of POME (before adding H₂O₂)

C_t = Final Concentration of POME (after reaction time t)

In addition to calculating the effectiveness of colour removal, biochemical oxygen demand (BOD) reduction was assessed. The BOD test, which was used to measure the oxygen depletion inside the POME over 3–7 days of incubation at 27°C, was a commonly used criterion for assessing the capacity of naturally occurring bacteria to digest organic materials (Soleimaninanadegani and Manshad, 2014). The BOD parameter is most utilized to assess the oxygen demand exerted by industrial effluent discharge on the receiving water body. BOD is an indirect measure of the presence of biodegradable organic compounds in water and can be employed to evaluate the efficacy of various treatment methods.

For the BOD test, the optimum concentration of H_2O_2 was applied and added to the sample of diluted POME before the upscaling UV/ H_2O_2 treatment. Two methods of H_2O_2 dosing were conducted in this experiment, including one-time and pulse dosing. For one-time dosing, H_2O_2 solution was added in one shot. For pulse dosing, H_2O_2 solution was added at a dosing rate of 0.3333 mL/min by adjusting the dropping rate of 50 mL burette at three drops per minute and 20 mL burette at one drop per minute. To improve the POME's thorough mixing when exposed to UV radiation, it has been vigorously mixed continuously using an aquarium air pump. The POME was continuously irradiated with a UV-C lamp for 12 hours, with samples taken every 1 hour for BOD analyses. The BOD testing was done following the BOD_3 standard, which requires three days and a temperature of $27^\circ C$. The dissolved oxygen in the samples on days 1 and 3 was measured using a PCD 650 Multi-parameter meter to assess the BOD. A best-fit line graph was then plotted to determine the trend of the BOD reduction rate of POME after UV/ H_2O_2 treatment with different dosing methods of H_2O_2 . According to the following formula, the BOD value and BOD efficiency were determined:

$$BOD = \frac{DO_0 - DO_3}{P} \quad (\text{Eq. 3.2})$$

$$BOD \text{ removal efficiency (\%)} = \frac{BOD_0 - BOD_t}{BOD_0} \times 100\% \quad (\text{Eq. 3.3})$$

DO_0 = Dissolved oxygen value at Day 1

DO_3 = Dissolved oxygen value at Day 3

P = Dilution factor/ Volume of sample used

BOD_0 = Initial concentration of BOD value of POME (before adding H_2O_2)

BOD_t = Final concentration of BOD value of POME (after reaction time t)

3.5 Parameter Studies

The degradation of diluted palm oil mill effluents (POME) by the UV/H₂O₂ system was monitored by various operating parameters, such as UV irradiation and H₂O₂ dosage methods. These process parameters were altered one after the other in this study, while the different process parameters stayed the same.

3.5.1 UV Irradiance

UV irradiation is a crucial factor that significantly influences the breakdown of contaminants in the UV/H₂O₂ system (Muruganandham and Swaminathan, 2006). The effectiveness of the treatment can be impacted by the quantity of UV lamps employed in a UV/H₂O₂ system. The number of UV lamps used will depend on various criteria, including the desired efficiency, the target pollutant, and the flow rate of the treated water. In this research work, different numbers of UV-C lamps (254 nm) were used to determine the degradation efficiency of POME by using UV/H₂O₂ systems at laboratory scale, such as 1 and 2 UV-C lamps (Mohammed, Alward, and S. Salman, 2020). The optimum number of UV-C lamps was employed at the pilot scale of the UV/H₂O₂ system.

3.5.2 H₂O₂ Dosage Ways

The primary capable species in the degradation process are the hydroxyl radicals (\bullet OH) generated from the direct photolysis of hydrogen peroxide (H₂O₂). This study evaluated and compared the efficacy of the UV/H₂O₂ treatment system H₂O₂ was dosed in one-time dosing and pulse dosing. A 50% H₂O₂ solution was used at 200, 300, 400, and 500 ppm concentrations, respectively, to test the effect of H₂O₂ concentration on the degrading process. The H₂O₂ solution was added to the POME sample in one shot for one-time dosing. The optimum concentration of H₂O₂ solution obtained from one-time dosing will be applied using both dosing methods, including one-time dosing and pulse dosing, to determine the optimum dosage ways of H₂O₂ solution. For pulse dosing, the H₂O₂ was added at a dosing rate of 0.3333 mL/min.

3.6 Upscaling UV/H₂O₂ System

A 200 L drum with an industrial UV light was used for an upscaling experiment in the engineering workshop. 180 L of a 100 ppm POME solution were put into the experiment's drum. The fluid flow at the bottom of the drum was encouraged using an aquarium air pump. The upscaling experiment employed two 300 W industrial UV lamps. The commercial UV light was inserted into the POME solution and screwed onto a piece of wood. The optimal H₂O₂ concentration was employed for the upscaling experiment, and natural pH was chosen despite pH 10 having a greater colour removal effectiveness than natural pH. It is due to the changing the pH of the POME solution before beginning the UV/H₂O₂ treatment would need additional chemical costs when used on an industrial scale, even if the efficacy of colour removal between pH 10 and natural pH is approximately the same (with a 3% efficiency difference). The upscaling experiment took place over 12 hours. Using a radiometer, the industrial UV lamp's light intensity was determined to be 17.94 mW/cm² for 254 nm and 0.815 mW/cm² for 365 nm. The schematic diagram and real configuration of a fully upscaling UV/H₂O₂ system are shown in Figures 3.4 and 3.5.

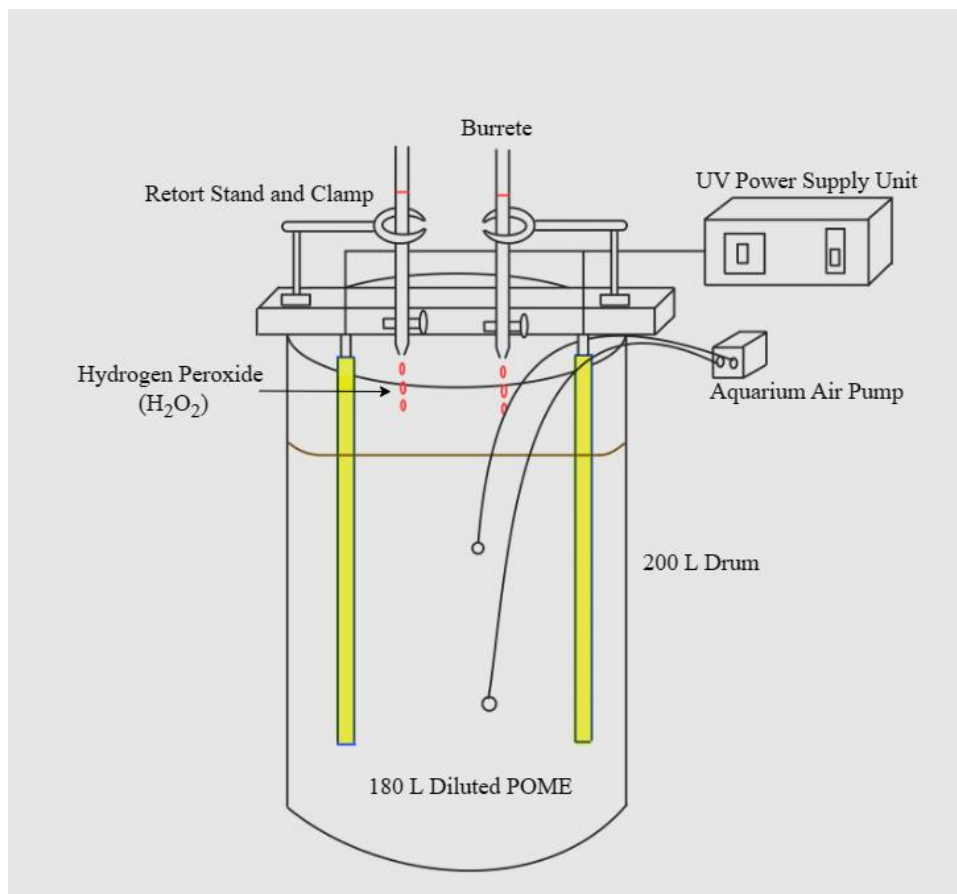


Figure 3.4: Schematic Diagram of Upscaling UV/H₂O₂ System



Figure 3.5: Side View of Upscaling UV/H₂O₂ System

3.7 Determination of Excess H₂O₂ using Redox Titration

To save the cost of UV/H₂O₂ treatment and prevent the scavenging effect during the treatment process, it is essential to determine the excess H₂O₂ concentration in the treated POME solution after the UV/H₂O₂ treatment. Thus, the redox titration via potassium permanganate (KMnO₄) was carried out to determine the excess H₂O₂ concentration in the treated POME solution. First and foremost, to standardize the KMnO₄ solution, 20 mL of sodium oxalate (0.05 M) was titrated using the KMnO₄ solution until the first permanent pink colour appeared. Next, 10 mL of the POME solution sample was transferred to a 500 mL beaker. Subsequently, the POME solution sample was mixed with 15 mL of 3 M sulfuric acid and 50 mL of deionized water. The solutions were titrated using standard KMnO₄ until the first permanent pink colour appeared. The volume of the standard KMnO₄ solution used to titrate the solutions was then recorded to calculate the excess H₂O₂ concentration in the treated POME solution. Figure 3.6 shows the setup of redox titration of POME solutions with a standard KMnO₄ solution.



Figure 3.6: Redox Titration with Standard KMnO₄ solution

3.8 Phytotoxicity Test

For the phytotoxicity evaluation, a comparison of the phytotoxicity of POME samples before and after photocatalytic degradation was conducted using mung bean (*Vigna radiata* L.) seed. For the experiment, mung bean seeds of a healthy, consistent size were used. They were deeply rinsed with distilled water following a 30-minute sterilisation process using a 0.5 (w/v)% NaOCl solution. Afterwards, each sterile petri dish (diameter of 90 mm) was equally filled with cotton pads and five selected mung bean seeds. A total of twelve consecutive days were spent at room temperature in three different petri dish setups, each of which was immersed in 5 mL of tap water (control), 5 mL of untreated POME solutions, and 5 mL of treated POME solutions at regular intervals of 12 hours. The procedure was modified and carried out based on the method published by Phang et al. (2021). After 12 days, the radicle lengths were measured and Equation (3.4) was used to evaluate the phytotoxicity of the POME samples (Aleksandra Dugandžić et al., 2017).

$$\text{Phytotoxicity (\%)} = \frac{(L_c - L_s)}{L_c} \times 100\% \quad (\text{Eq. 3.4})$$

L_c = Radicle length of control

L_s = Radicle length of samples

CHAPTER 4

RESULTS AND DISCUSSION

The experimental results of the research investigation are summarized in this chapter. In the first section of this chapter, four sets of control experiments with different conditions were carried out using the lab scale and upscaling UV/H₂O₂ treatment on the POME treatment to ensure that the results obtained are not just random events. The following section covered the impact of various operating parameters on the UV/H₂O₂ process at the lab scale. These parameters included the number of UV lights and the concentration of H₂O₂. In the third section, the performance of the UV/H₂O₂ advanced oxidation processes (AOPs) was then examined through the final discharge POME's BOD reduction rate under a range of operating conditions, such as the number of UV lights and the H₂O₂ dosage (one-time dosing vs. pulse dosing). To lower the quantity of H₂O₂ utilized and save treatment costs for the UV/H₂O₂ system on the POME treatment, the determination of excess H₂O₂ during the entire UV/H₂O₂ process was covered in the following part. Lastly, a phytotoxicity test will be performed to assess the toxicity of the treated POME on the environment by examining its effects on the germination and growth of mung bean seeds.

4.1 Control Experiment

Before the different effects of operating parameter studies were carried out, four sets of control experiments for lab scale and upscaling UV/H₂O₂ treatment were conducted. Controls serve as a benchmark and are frequently employed as precautions against internal variables that could affect an experiment's conclusion. The control experiments were conducted under various conditions, including only POME, UV Light, POME with H₂O₂, and the UV/ H₂O₂ treatment. All control experiments were performed with the fixed concentration of POME (100 ppm), and the H₂O₂ (400 ppm) was utilized. Figure 4.1 shows the BOD reduction and colour removal efficiency of POME for the four control experiments. No decolourization and BOD reduction effect occurred for the control experiments with only POME since there was no reaction without UV light and H₂O₂. The UV light alone did not lead to colour removal and BOD reduction in POME due to the challenging nature of breaking down these organic compounds, including lignin, cellulose, and phenolic compounds, necessitating highly reactive oxides for effective degradation. Applying UV light degraded the contaminants but takes too long; dyeing and degradation rates rose with lamp intensity, and UV power was correlated with pseudo-first-order reaction rates (Shu and Chang, 2005).

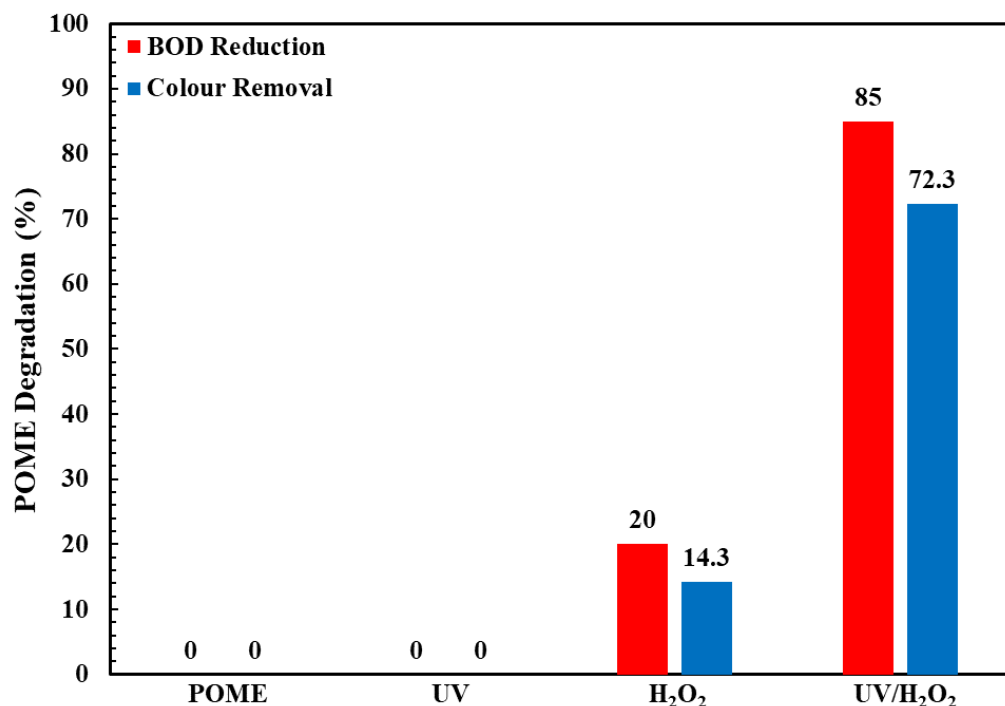


Figure 4.1: BOD Reduction and Colour Removal Efficiency of POME for The Various Conditions of Control Experiment

With the only presence of H₂O₂, the colour removal efficiency of the POME was 14.3%, and the BOD of the POME can be reduced by 20%. Lescano et al. (2012) state that if saturated oxygen is present in the solution, organic contaminants can be photolyzed and degraded by H₂O₂. Although the efficiency of this process is relatively low, Kim and Nriagu (2000) also discovered that the organic pollutants arsenic (III) can be oxidized with dissolved air in water. With the presence of UV and H₂O₂, the colour removal efficiency reached 72.3% in the lab scale of UV/H₂O₂ treatment, and the BOD reduction was 85% for the upscaling UV/H₂O₂ treatment. The photolysis of H₂O₂ occurred with UV light, resulting in the generation of •OH with a standard redox potential of 2.77 V, much higher than H₂O₂. The organic pollutants in POME can be attacked by •OH and undergo further degradation to form CO₂, H₂O, and mineral acids (Ainhoa Rubio-Clemente, Chica, and Peñuela, 2017).

4.2 Effect of Operating Parameter in Lab Scale UV/H₂O₂ Treatment

4.2.1 Hydrogen Peroxide Concentration

The effect of the concentration of hydrogen peroxide (H₂O₂) on the POME treatment using the lab scale UV/H₂O₂ with one-time dosing of H₂O₂ was studied. The decolourization efficiency of POME performed with various concentrations of H₂O₂ as shown in Figure 4.2. The decolourization efficiency of POME increased from 56.1% to 64.1% when the H₂O₂ concentration increased from 200 ppm to 400 ppm. The decolourization rate was minimal because H₂O₂ cannot produce enough hydroxyl radicals (\bullet OH) at low concentrations. Increasing the H₂O₂ concentration caused more \bullet OH to be made at low peroxide levels, speeding up the pace at which POME degrades (Zang and Farnood, 2005). When the H₂O₂ concentration increased from 400 to 500 ppm, the colour removal efficiency decreased from 64.1% to 41.1%.

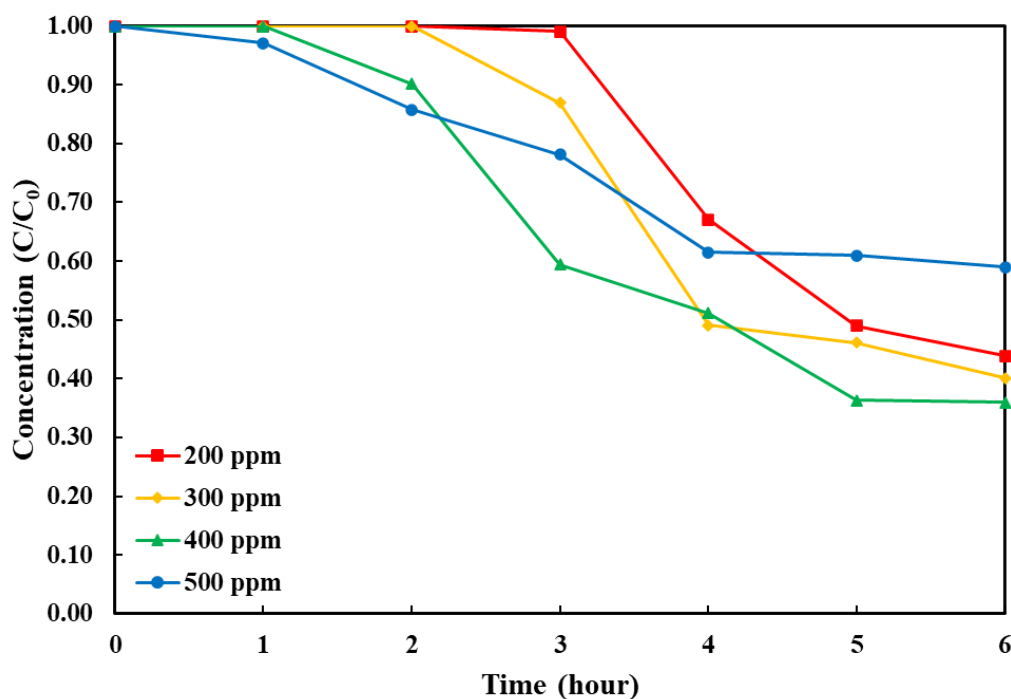
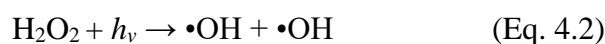


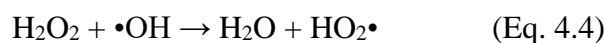
Figure 4.2: Effect of Different Concentrations of H₂O₂ on POME with One UV Light ([POME] = 100 mg/L, [H₂O₂] = 400 mg/L)

According to Alkan et al. (2007) and Elmorsi et al. (2010), hydrogen peroxide can produce potent $\bullet\text{OH}$ by functioning as an electron acceptor in Equation (4.1). Equation (4.2) shows two $\bullet\text{OH}$ can be produced when hydrogen peroxide absorbs UV radiation.



As shown in Figure 4.2, the colour removal efficiency rose as hydrogen peroxide concentration increased from 200 ppm to 400 ppm. However, the efficiency of the degradation might be reduced due to the higher H_2O_2 concentration. Based on the results depicted in Figure 4.2, the colour removal efficiency decreased as H_2O_2 concentration increased from 400 ppm to 500 ppm. This is because the OH free radicals generated during H_2O_2 photolysis can react with both excess H_2O_2 and POME organic pollutants. The decolourization process is inhibited by competitive reactions caused by large concentrations of $\bullet\text{OH}$ radicals and excess hydrogen peroxide (Aleboyeh, Moussa, and Aleboyeh, 2005).

Therefore, the excess H_2O_2 concentration resulted in a scavenging effect. The scavenging action observed in Equations (4.3) and (4.4) may be the consequence of the auto-decomposition of hydrogen peroxide into oxygen and water as well as the recombination of hydroxyl radical (Buthiyappan, Abdul Aziz, and Wan Daud, 2015).



Therefore, excess H_2O_2 can function as a scavenger of $\bullet\text{OH}$ and, by interacting with radicals or being adsorbed at the catalyst surface, it can compete with organic molecules and reduce treatment efficacy (Neyens and Baeyens, 2003). The effectiveness of the treatment will be reduced if the H_2O_2 dose is too low, as this will also result in a low $\bullet\text{OH}$ arrangement. Therefore, the optimal H_2O_2 concentration for the UV/ H_2O_2 treatment for POME was determined, which was 400 ppm.

4.2.2 Number of UV Light

The number of UV lights played a significant role in boosting the performance of the lab-scale UV/H₂O₂ system. Different numbers of UV light were used in the lab scale UV/H₂O₂ treatment with one-time dosing of H₂O₂ to determine the effect of the number of UV lights on the POME decolourization efficiency. Figure 4.3 depicts the UV/H₂O₂ system's performance in decolourizing the POME using different numbers of UV lights. Based on Figure 4.3, the decolourization efficiency of POME enhanced as the number of UV lights used increased from one to two. The POME degradation efficiency under one UV light was 64.1%, while the efficiency increased to 72.3% when two UV lights were applied in the UV/H₂O₂ system.

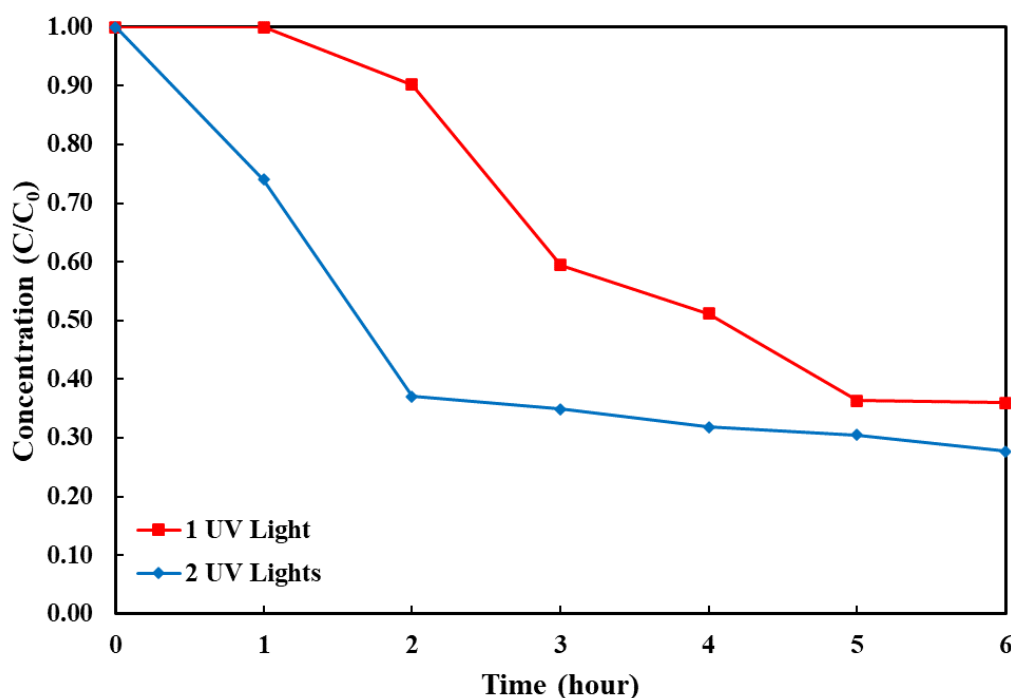


Figure 4.3: Decolourization Efficiency of POME at Various Numbers of UV Lights with One-time Dosing of H₂O₂ ([POME] = 100 mg/L, [H₂O₂] = 400 mg/L)

It was due to the significant rise in energy from ultraviolet light, which was responsible for breaking the bonds within organic compounds. This process created highly reactive radical intermediates, while reducing the concentration of the original organic compounds (Macawile et al., 2011). The rapid decline in POME concentration within the initial three hours of photolytic reaction can be attributed to the formation of $\bullet\text{OH}$. In other words, the photodegradation of H_2O_2 produced more hydroxyl radicals, which in turn caused more POME to be degraded within the UV/ H_2O_2 system. Conversely, the relatively steady degradation of POME observed after the fourth hour can be attributed to the absorption of UV light not only by POME itself but also by the intermediate products generated during the photodegradation process (Macawile et al., 2011). The rise in photodegradation efficiency of the applied light energy mirrored findings from studies on the photo destruction of acid orange 7 (Behnajady, Modirshahla, and Shokri, 2003), reactive azo dye (Muruganandham and Swaminathan, 2004), and 4-chloro-3,5-dinitrobenzoic acid (Lopez et al., 2000).

4.3 Effect of Operating Parameter in Upscaling UV/H₂O₂ Treatment

4.3.1 Number of UV Light

In the upscaling UV/H₂O₂ treatment, the power required for the POME degradation was optimized for an energy-efficient process by considering the number of 254 nm UV-C lamps with one-time dosing of H₂O₂. Figure 4.4 illustrates the BOD reduction of POME at different numbers of UV lights with one-time dosing of H₂O₂. As shown in the Figure 4.4, 62% of the BOD was found to be reduced under one UV-C light, which was from 100 to 38 mg/L of BOD. However, with the increase in the number of lamps from one to two, the photolysis performance reached 75%. The BOD reduction under two UV lights reduced the BOD from 100 to 25 mg/L. Increasing the number of UV lamps will provide more energy for the •OH to be generated, and the reaction time will also be lowered, which was thought to have the most significant impact on POME degradation (Mohammed, Alward, and S. Salman, 2020). It was clearly shown that 53% of BOD could be reduced at the 6th hour of treatment under two UV lights, while only 28% of BOD was reduced under one UV light. As the number of UV lights increased, the overall light intensity increased as well, subsequently improving the BOD reduction efficiency of POME. This was due to the higher generation of •OH. The rate at which H₂O₂ was photolyzed was restricted at low UV power, while the rate at which H₂O₂ was photo-dissociated increases with increasing UV power due to forming more •OH (Modirshahla and Behnajady, 2006). The hydroxyl radicals created by the UV/H₂O₂ reaction oxidize the organic pollutants, which breaks them down into simpler, biodegradable compounds. This produced an effluent that may be useful to microorganisms because the pollutant load has dropped to a point where biodegradation processes can take place, further lowering the pollutant load (Urbina-Suarez et al., 2023).

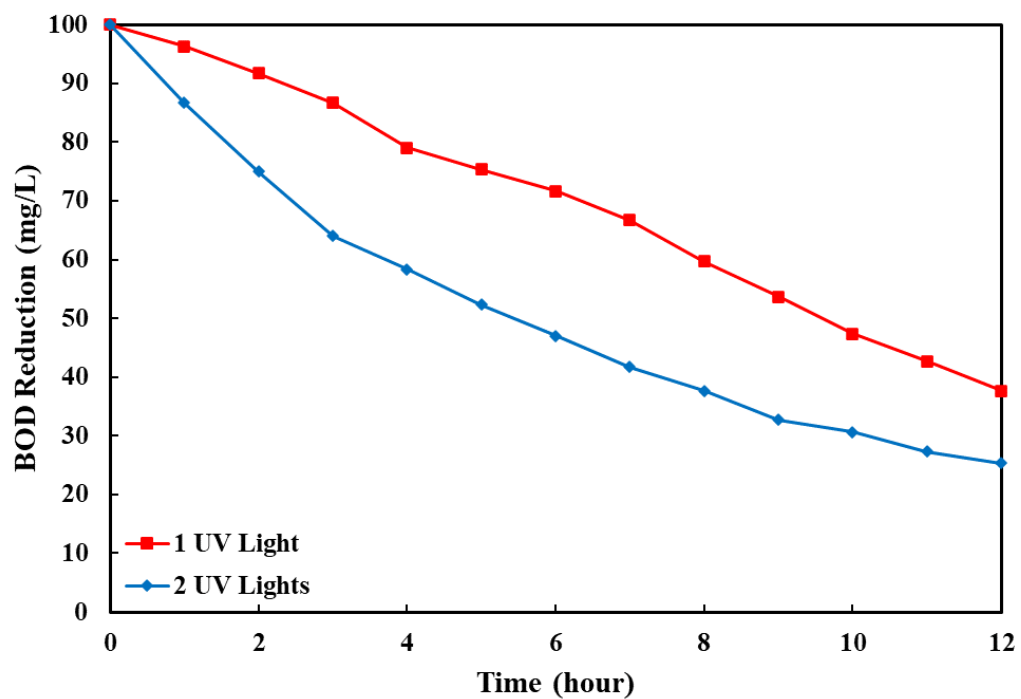
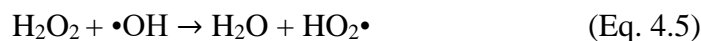


Figure 4.4: BOD Reduction of POME at Different Numbers of UV Lights with One-time Dosing of H_2O_2 ($[\text{POME}] = 100 \text{ mg/L}$, $[\text{H}_2\text{O}_2] = 400 \text{ mg/L}$)

4.3.2 One-time Dosing vs Pulse Dosing of H₂O₂

Figure 4.5 shows the BOD reduction of POME at various dosing methods with 2 UV lights. As shown in Figure 4.5, with the optimum parameters of 2 UV lights and pulse dosing of 400 mg/L of H₂O₂, the treatment yielded the most significant reduction in BOD (85%) and colour (88.4%) in the samples. This kind of UV/H₂O₂ treatment setting has successfully satisfied the requirement of DOE as the BOD can be reduced to 15 mg/L after 12 hours of treatment duration. However, the method with a one-time dosing under the same conditions was less efficient (75% BOD reduction). One possible explanation could be that the treatment's initial 400 mg/L H₂O₂ concentration becomes too high, lowering the process's efficiency. The reaction bulk's initial high concentration of H₂O₂ and the accompanying high radical production can result in a surplus of H₂O₂, which can serve as a source for •OH radicals to be captured (Equation 4.4). The intermediates that are formed can then compete with the organic materials in POME for the •OH radical (Almeida et al., 2015). The graph shows that BOD reduction happens quickly in the first two hours of treatment and then at a slower rate in the remaining hours. Many of the organic material's breakdown products are thought to have been produced by intermediaries, which were created by the photolysis of H₂O₂ molecules in •OH radicals (Equation 4.5). The •OH radicals are competitively attracted to the produced intermediaries, which can have a more complicated chemical structure and impede their destruction (Almeida et al., 2015). This could explain why, despite adding H₂O₂, the BOD drop was sluggish in the 10 hours of treatment.



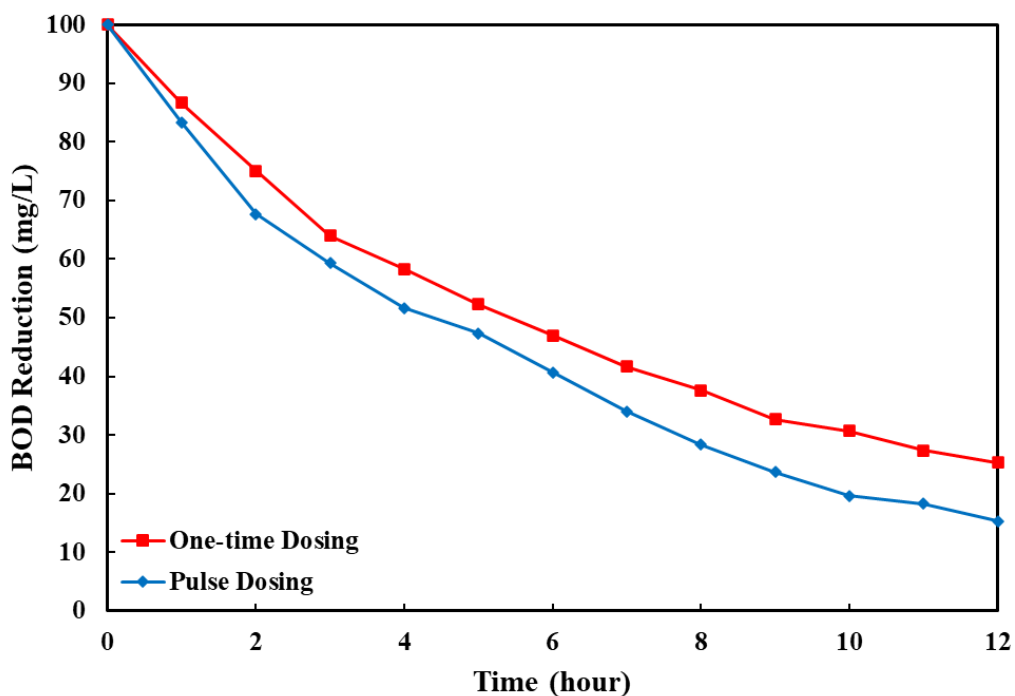


Figure 4.5: BOD Reduction of POME at Different Dosing Methods with 2 UV Lights ($[POME] = 100 \text{ mg/L}$, $[H_2O_2] = 400 \text{ mg/L}$, Pulse Dosing Rate = 0.3333 mL/min)

The degradation of POME by upscaling UV/H₂O₂ treatment with various dosing methods is shown in Figure 4.6. POME's pseudo-first-order rate constant (k') was 0.1209 hour^{-1} by one-time dosing and increased to 0.1575 hour^{-1} by pulse dosing. These findings unequivocally showed that UV/H₂O₂ applied with pulse dosing of H₂O₂ was a more efficient method of removing organic substances in POME than one-time dosing of H₂O₂. The data indicated that the BOD reduction rate of POME rose progressively with pulse dosing of H₂O₂, as shown in Figure 4.7. However, the relationship was not linear. The enhanced $\bullet\text{OH}$ in solution at pulse dosing of H₂O₂ under the same number of UV lights was likely responsible for the observed results. With the application of pulse dosing, POME's degradation rate significantly increased. An excellent linear fit ($R^2 = 0.9968$, with $k' = 0.1575$ as the fitting equation) indicated that k' was precisely proportional to the dosing rate. This relationship suggested the vital role of the H₂O₂ dosing method. Pulse dosing of H₂O₂ can produce many more radicals due to H₂O₂'s improved photolysis.

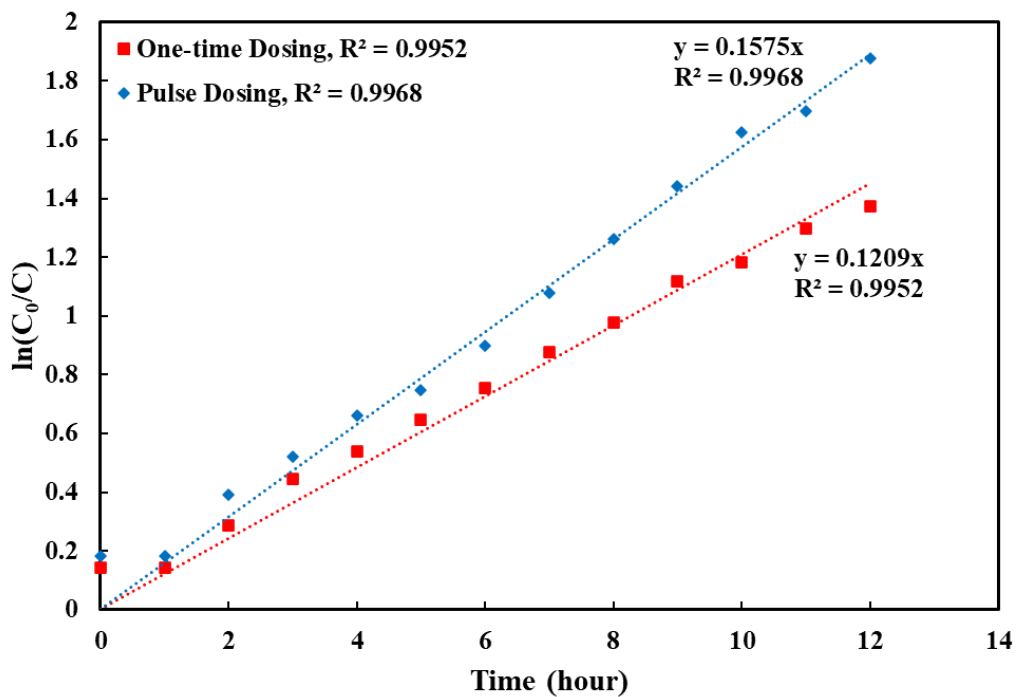


Figure 4.6: Pseudo-First-Order Kinetics Plot of POME Degradation During UV/H₂O₂ Process with Different Dosing Methods ([POME] = 100 mg/L, [H₂O₂] = 400 mg/L, Pulse Dosing Rate = 0.3333 mL/min)

4.3.3 Pulse Dosing of H₂O₂ vs Pulse Dosing of H₂O₂ with 3 Hours Dark

To reduce the operating cost of the experiment, another UV/H₂O₂ treatment was carried out with 2 UV lights and the pulse dosing of H₂O₂ on the condition that the first three hours were dark. In such situations, a photo-oxidation reaction occurs without UV lights. Figure 4.7 shows the BOD reduction of POME by UV/H₂O₂ treatment in different conditions. As illustrated in Figure 4.7, the UV/H₂O₂ treatment with the first three hours of UV lights switched off has a relatively low efficiency, reducing the BOD of POME to 19 ppm. Although both treatment methods could successfully reduce the BOD of POME to below 20 ppm and satisfy the requirements set by DOE, there was no doubt that the UV/H₂O₂ with 12 hours of UV lights switched on has higher performance in degrading the POME.

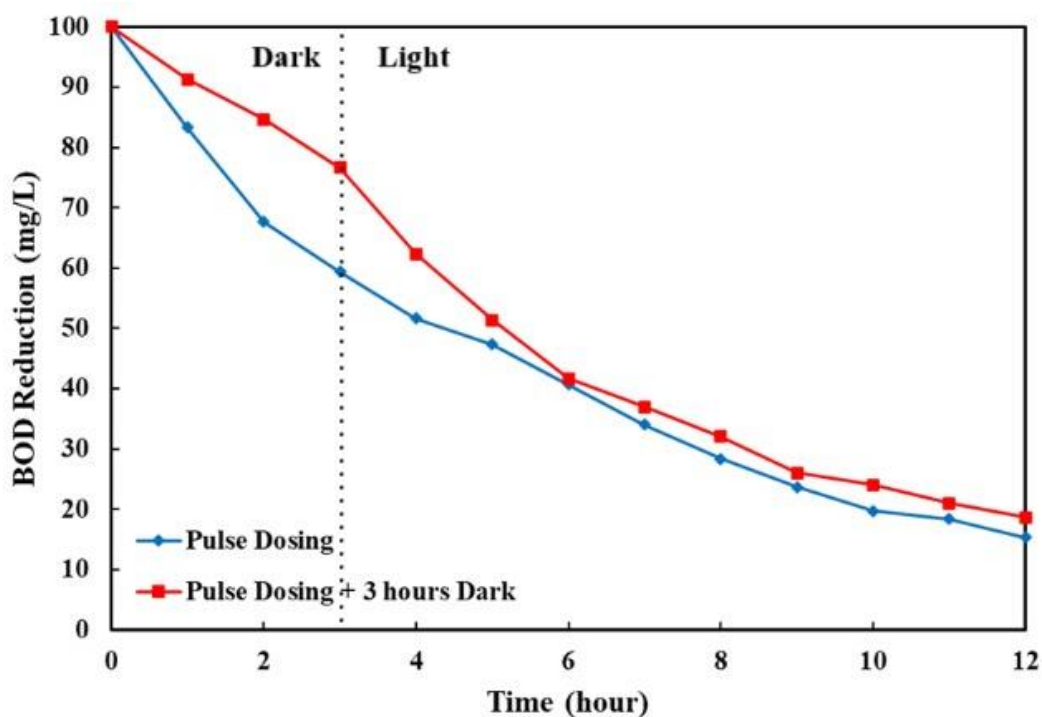


Figure 4.7: BOD Reduction of POME at Different Conditions of Pulse Dosing with 2 UV Lights ([POME] = 100 mg/L, [H₂O₂] = 400 mg/L, Pulse Dosing Rate = 0.3333 mL/min)

Once more, the role of H_2O_2 in the reaction process should be considered, even if the conversions of POME degraded by H_2O_2 are minimal. It should be considered that the percentage of POME degradation would rise even further with longer reaction times (Lescano et al., 2012). This case is similar to the previous explanation for oxygen oxidation in Section 4.1. Ultimately, this response may be insignificant. There has been prior documentation of organic pollutants like As (III) being directly oxidized by direct H_2O_2 (Pettine, Campanella, and Millero, 1999). According to this publication, the pH in place significantly impacts the reaction, leading to the emergence of many dominating species that are thermodynamically capable of oxidizing.

In wastewater treatment, the biochemical oxygen demand (BOD) is one of the most significant and often used parameters for describing the organic pollution of water and wastewater, which is determined by the amount of oxygen needed by aerobic microbes to break down organic materials in wastewater (Verma and Singh, 2013). Assessing the extent of the photocatalytic process for additional effluent characteristics, such as pH, $\text{NH}_3\text{-N}$, turbidity, and COD, was also critical. Table 4.1 summarizes the analyzed quality parameters of diluted POME before UV/ H_2O_2 treatment for degradation before and after photolysis. As indicated in Table 4.1, there was a significant decrease in the pre-treated POME wastewater parameters assessed following a 12-hour UV/ H_2O_2 treatment. As shown in Table 2.2, the proposed UV/ H_2O_2 system used in this study treated POME wastewater, and the quality parameter was found to be below the water quality threshold limitations set by the Malaysian Department of Environment (DOE). Therefore, the proposed UV/ H_2O_2 system offered a viable alternative for broader application as an eco-friendly way of degrading pre-treated POME wastewater.

Table 4.1: A Summary of the Analysed Quality Parameters of Diluted POME Prior to UV/H₂O₂ Treatment for Degradation Before and After Photolysis Under UVC Light with Hydrogen Peroxide Oxidant ([POME] = 100 ppm, [H₂O₂] = 400 ppm, Pulse Dosing Rate = 0.3333 mL/min, UVC Light Irradiation Time = 12 hours)

Parameter	Before Treatment	After Treatment	Efficiency (%)
BOD ₃ (mg/L)	192.5	15	92.2
COD (mg/L)	1810	116	93.6
NH ₃ -N (mg/L)	33	28	15.2
Turbidity (NTU)	7.54	3.6	52.3
pH	7.92	7.61	-

4.4 Determination of Excess H₂O₂

As a well-known strong oxidant, hydrogen peroxide (H₂O₂) was widely used in advanced oxidation processes (AOPs) to break down several kinds of organic compounds, one of which was phenol (Alnaizy and Akgerman, 2000; Esplugas et al., 2002; Ghaly et al., 2001; Pera-Titus et al., 2004). UV light was used in this process to photolyze H₂O₂ directly. The reason the •OH radicals were so reactive because they could harm organic molecules with minimal bias. Despite the possibility that this reaction occurs naturally, it was previously established that H₂O₂ was toxic in quantities that might harm a wide range of organisms when utilized in excess. Developing more potent techniques to remove it from the environment remained essential (Silva et al., 2007). The amount of H₂O₂ in the POME solution after the 12-hour UV/H₂O₂ process is displayed in Figure 4.8.

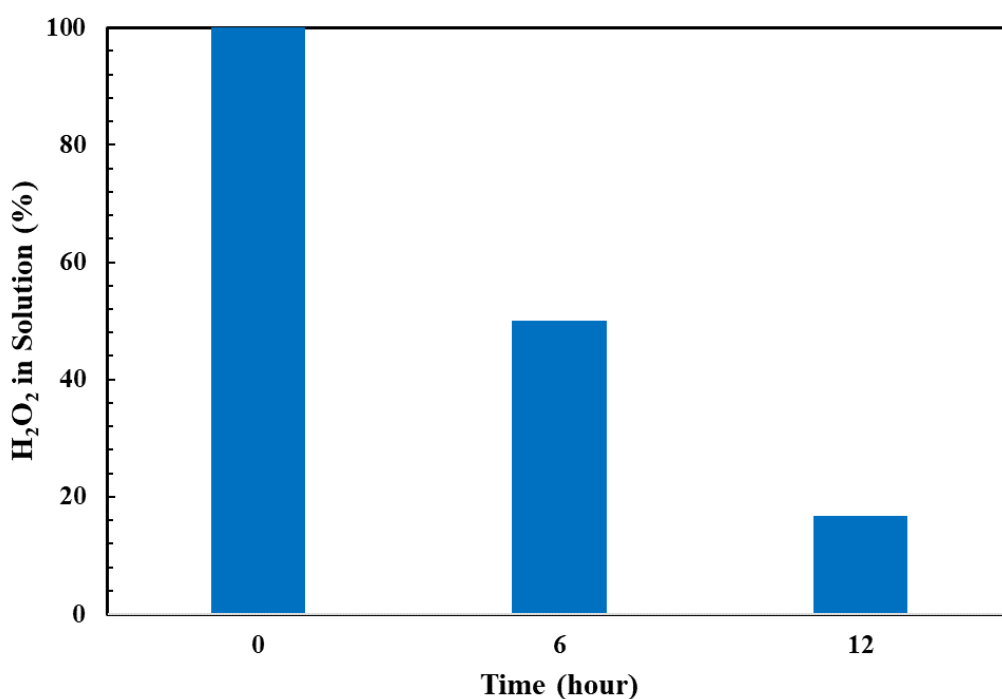
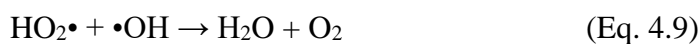
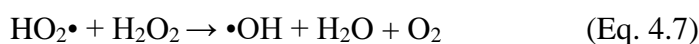


Figure 4.8: Amount of H₂O₂ in Excess in POME Solution after 12 hours of UV/H₂O₂ Treatment ([POME] = 100 mg/L, [H₂O₂] = 400 mg/L, Pulse Dosing Rate = 0.3333 mL/min)

As depicted in Figure 4.8, 16.7% H₂O₂ was in excess after 12 hours of POME degradation by using UV/H₂O₂ treatment. Based on the findings of Nogueira et al. (2016), raising the H₂O₂ concentration can enhance the efficiency of the degradation of organic pollutants. Since both the catalyst and the excess H₂O₂ contribute to the formation of oxidizing species, excess H₂O₂ may generate additional hydroxyl radicals, which may improve the oxidation and removal of organic pollutants (Ahmed et al., 2010). However, the H₂O₂ in excess can act as the radical scavenger as it could be attributed to the auto-decomposition of H₂O₂ into oxygen and water or the self-quenching of OH radicals by more H₂O₂, which resulted in the production of HO₂• radicals based on Equations (4.5 – 4.9) (Ghaly et al., 2001; Movahedian, Mohammadi, and Asadi, 2009; Ku, Tu, and Ma, 2005).



When the quantity of H₂O₂ increased, the reaction rate decreased because HO₂• was less reactive than •OH (Zang and Farnood, 2005). The higher consumption of the chemical reagent caused by excess H₂O₂ might lead to increased operational costs. Before discharge or continued usage, extra procedures, or treatment methods, such as catalytic decomposition of H₂O₂ with the addition of heat and sodium carbonate (Na₂CO₃), activated carbon adsorption and electrochemical reduction/oxidation, can be necessary to eliminate any remaining H₂O₂ (Wu and Englehardt, 2012; Wang et al., 2021; Dakubo, Baygents, and Farrell, 2012). Thus, it was essential to apply the optimum concentration of H₂O₂ to increase the efficiency of the UV/H₂O₂ process and lower treatment expenses.

4.5 Cost Analysis

Considering the UV/H₂O₂ system's economics and effectiveness in degrading the treated POME was critical. Thus, this section examined the cost of setting up the UV/H₂O₂ system. The bill was produced in accordance with Tenaga Nasional Berhad's (TNB) implementation of the Low Voltage Industrial Tariff. The total cost of electricity for the UV/H₂O₂ system is shown in Table 4.2, whereas the total expenses of materials utilized for the treated POME degradation are listed in Table 4.3. To make the cost analysis simpler, the following five assumptions were made (Yu et al., 2020):

- i) The costs of electricity, H₂O₂, and UV lamp replacement made up the total operational cost.
- ii) Labor costs were not considered in this model.
- iii) The market prices for H₂O₂, electricity, and UV lamps were constant.
- iv) The lifetime and efficiency of the lamps were also constant.
- v) There was minimal variation in the UV radiation from the lamps over their lifetime.

Using Equation (4.10) as provided by Martinez, Ebenhack, and Wagner (2019), the power usage was computed as below:

$$\text{Electricity Consumption (kWh)} = \frac{\text{Power (W)} \times \text{Operation Hour (h)}}{1000} \quad (\text{Eq. 4.10})$$

Table 4.2: Cost and Total Electricity Used for the UV/H₂O₂ System

Equipment	Power (W)	Duration (h)	Total Consumption (kWh)
UV-C Lamp	600	12	7.2
Aquarium Air Pump	3	12	0.036
Total			7.236

$$\begin{aligned} \text{Total Cost of Electricity} &= 7.236 \text{ kWh} \times \text{RM } 0.38 / \text{kWh} \\ &= \text{RM } 2.75 \end{aligned}$$

Table 4.3: Total Cost of Material for POME Degradation by UV/H₂O₂ System

Material	Quantity	Unit	Unit Price (RM)	Price (RM)
H ₂ O ₂	120	mL	0.0115	1.38
Total				1.38

$$\begin{aligned}
 \text{Overall Production Expense} &= \text{Total Cost of Electricity} + \text{Total Cost of Material} \\
 &= \text{RM } 2.75 + \text{RM } 1.38 \\
 &= \text{RM } 4.13
 \end{aligned}$$

The UV/H₂O₂ system used in this study had an overall production cost of RM 4.13. Approximately 67% of the total cost was related to the electricity used in the UV/H₂O₂ system. Alternatively, the UV/H₂O₂ system was designed to breakdown organic contaminants into water and oxygen alone, leaving no toxic residues behind, and it was meant to be extensively utilized as an eco-friendly alternative for treating pre-treated POME wastewater. As a prerequisite to reducing the cost of the built UV/H₂O₂ system and further supporting the system's economic viability, optimizing variables such as H₂O₂ concentration, UV radiation applied, and contact time between the wastewater and the light for each type of organic pollutant was essential.

4.6 Phytotoxicity Evaluation

To encourage the reusability of treated POME, evaluation of the environmental impact of actual POME treatment and its potential application in field irrigation is crucial. Figure 4.10 depicts the phytotoxicity of treated and untreated POME solutions using mung bean seeds. When compared to the control (0%), it was clear that the untreated POME showed an initial phytotoxicity of 63.7%. The phytotoxicity in the treated POME was significantly decreased to 19.7% following the UV/H₂O₂ treatment. The length of the mung bean's radicles also showed a decline in phytotoxicity. Before and after the UV/H₂O₂ treatment, the average radicle lengths of mung beans were 11.5 and 5.2 cm, respectively. The outcomes demonstrated a significant reduction in phytotoxicity following the UV/H₂O₂ treatment, suggesting the effectiveness of the UV/H₂O₂ system in lowering phytotoxicity in POME wastewater. Figure 4.10 shows the germination of mung bean seeds with three various solutions after 12 days.

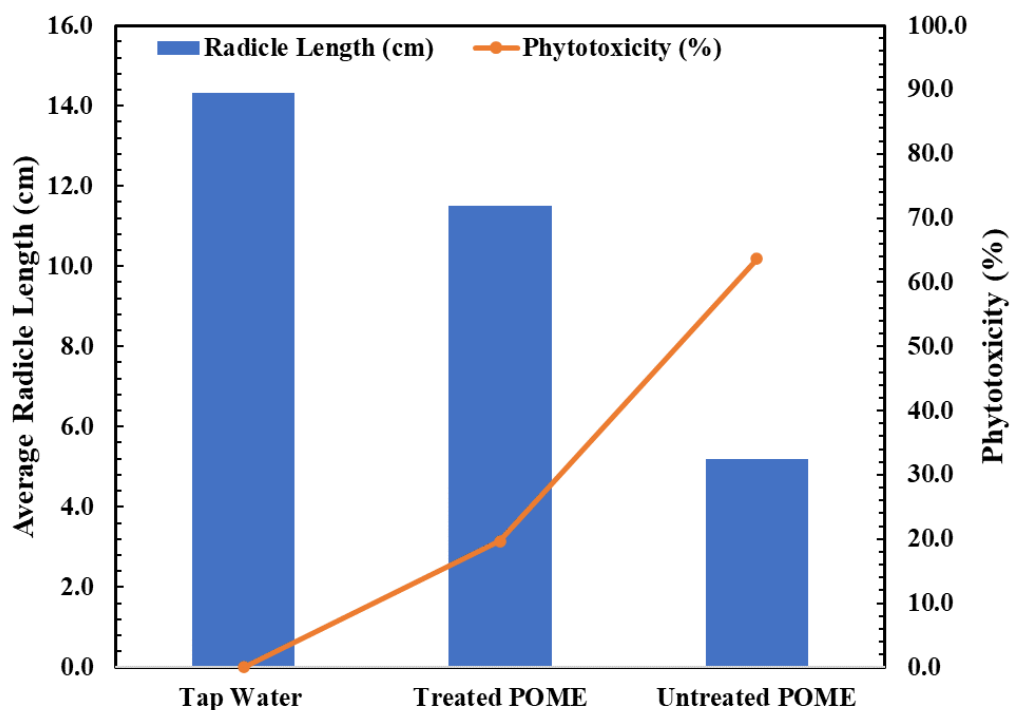


Figure 4.9: Phytotoxicity tests of POME before and after UV/H₂O₂ Treatment



Figure 4.10: Mung Bean Seeds Germination after 12 days: (a) Control (Tap Water); (b) Before Treatment (Untreated POME); (c) After Treatment (Treated POME)

CHAPTER 5

CONCLUSION AND RECOMMENDATIONS

5.1 Conclusion

In the present research, the utilization of UV/H₂O₂ treatment for the degradation of palm oil mill effluent (POME) demonstrates its effectiveness in achieving high colour removal (up to 88.4%) and BOD reduction from 100 ppm to 15 ppm (up to 85%) in 12 hours by optimizing critical operating parameters. In other words, it successfully achieved the objectives of this study, and it accomplished the requirements set by the Department of Environment (DOE), which was to reduce the BOD of pretreated POME to below 20 ppm. The H₂O₂ concentration and the number of UV lamps played essential roles, with an optimal H₂O₂ concentration of 400 ppm and two UV lamps providing the best results. Pulse dosing of H₂O₂ was more effective than one-time dosing, increasing the pseudo-first-order rate constant. The optimized UV/H₂O₂ system (two UVC lights; 400 ppm of H₂O₂, 0.3333 mL/min of pulse dosing rate) met regulatory requirements and significantly reduced the phytotoxicity of the treated POME. While the total operating cost was estimated at RM 4.13, with electricity being the major contributor, it is essential for further optimization to improve the economic viability of this eco-friendly POME wastewater treatment method. Lastly, this study helps achieve Sustainable Development Goal No. 6, Clean Water and Sanitation, to safeguard water-related ecosystems and their biodiversity by ensuring their availability and sustainable management.

5.2 Recommendations for Future Studies

Upon completion of the present study, several essential elements were recommended to be considered in future UV/H₂O₂ photolysis oxidation studies:

- a) The study should assess the influence of pH, temperature, and initial POME characteristics (e.g., COD, colour, turbidity) on the performance of the UV/H₂O₂ process and optimize these operating conditions to enhance the treatment efficiency further.
- b) It is suggested to investigate the synergistic effects of combining UV/H₂O₂ with other advanced oxidation processes (e.g., ozonation, Fenton's reaction) or biological treatment methods and evaluate the feasibility and performance of a hybrid treatment system for comprehensive POME degradation and resource recovery.
- c) The potential applications of the treated POME, such as irrigation, fertilizer production, or the extraction of valuable compounds (e.g., phenolics, carotenoids), should be explored to assess the quality and safety of the treated POME for these alternative uses.

REFERENCES

- Abu, S., Hassimi Abu Hasan, Abdul Wahab Mohammad, Sheikh, R., Teow Yeit Haan, Rahmat Ngteni and Khairul Aimi Yusof, 2018. A review of moving-bed biofilm reactor technology for palm oil mill effluent treatment. *Journal of Cleaner Production*, [e-journal] 171, pp. 1532–1545. <https://doi.org/10.1016/j.jclepro.2017.10.100>.
- Affam, A.C. and Bin Bistar, A.R., 2020. Oxidation of palm oil mill effluent using hydrogen peroxide and catalysed by UV light/zinc oxide. *IOP Conference Series: Materials Science and Engineering*, [e-journal] 736, p. 042025. <https://doi.org/10.1088/1757-899x/736/4/042025>.
- Ahmad, A.L. and Chan, C.Y., 2009. Sustainability of palm oil industries: An innovative treatment via membrane technology. *Journal of Applied Sciences*, [e-journal] 9, pp. 3074–3079. <https://doi.org/10.3923/jas.2009.3074.3079>.
- Ahmed, S., Rasul, M.G., Martens, W.N., Brown, R. and Hashib, M.A., 2010. Advances in heterogeneous photocatalytic degradation of phenols and dyes in wastewater: A review. *Water, Air, & Soil Pollution*, [e-journal] 215, pp. 3–29. <https://doi.org/10.1007/s11270-010-0456-3>.
- Ainhoa Rubio-Clemente, Chica, E. and Peñuela, G.A., 2017. Kinetic modelling of the UV/H₂O₂ process: Determining the effective hydroxyl radical concentration. *InTech eBooks*, [e-journal]. <https://doi.org/10.5772/65096>.
- Akhbari, A., Kutty, P.K., Chuen, O.C. and Ibrahim, S., 2019. A study of palm oil mill processing and environmental assessment of palm oil mill effluent treatment. *Environmental Engineering Research*, [e-journal] 25. <https://doi.org/10.4491/eer.2018.452>.
- Aleboye, A., Moussa, Y. and Aleboye, H., 2005. The effect of operational parameters on UV/H₂O₂ decolourisation of Acid Blue 74. *Dyes and Pigments*, [e-journal] 66, pp. 129–134. <https://doi.org/10.1016/j.dyepig.2004.09.008>.

- Aleksandra Dugandžić, Tomašević, A.V., Maja Radišić, Šekuljica, N.Ž., Mijin, D.Ž. and Petrović, S.D., 2017. Effect of inorganic ions, photosensitisers, and scavengers on the photocatalytic degradation of nicosulfuron. *Journal of Photochemistry and Photobiology A-chemistry*, [e-journal] 336, pp. 146–155. <https://doi.org/10.1016/j.jphotochem.2016.12.031>.
- Alhaji, M.H., Sanaullah, K., Lim, S.F., Khan, A., Hipolito, C.N., Abdullah, M.O., Bhawani, S.A. and Jamil, T., 2016. Photocatalytic treatment technology for palm oil mill effluent (POME) – A review. *Process Safety and Environmental Protection*, [e-journal] 102, pp. 673–686. <https://doi.org/10.1016/j.psep.2016.05.020>.
- Almeida, Caio Vinícius da S., Macedo, Matheus S., Eguiluz, Katlin Ivon B., Salazar-Banda, Giancarlo R., Queissada, Daniel D., 2015. Indanthrene blue dye degradation by UV/H₂O₂ process: H₂O₂ as a single or fractioned aliquot?. *Environmental Engineering Science*, [e-journal] 32, pp. 930–937. <https://doi.org/10.1089/ees.2015.0171>.
- Alnaizy, R. and Akgerman, A., 2000. Advanced oxidation of phenolic compounds. *Advances in Environmental Research*, [e-journal] 4, pp. 233–244. [https://doi.org/10.1016/S1093-0191\(00\)00024-1](https://doi.org/10.1016/S1093-0191(00)00024-1).
- Andrades, J.A., Lojo-López, M., Egea-Corbacho, A. and Quiroga, J.M., 2022. Comparative effect of UV, UV/H₂O₂ and UV/H₂O₂/Fe on terbuthylazine degradation in natural and ultrapure water. *Molecules*, [e-journal] 27, p. 4507. <https://doi.org/10.3390/molecules27144507>.
- Anwar, F. and Arthanareeswaran, G., 2019. Silver nanoparticle coated hydroxyapatite nano-composite membrane for the treatment of palm oil mill effluent. *Journal of Water Process Engineering*, [e-journal] 31, p. 100844. <https://doi.org/10.1016/j.jwpe.2019.100844>.
- AWC, n.d. *Advanced oxidation processes*. [Online] Available from: [https://www.membranechemicals.com/water-treatment/advanced-oxidation-plants/#:~:text=Advanced%20oxidation%20processes%20\(abbreviation%3A%20AOPs,hydroxyl%20radicals%20\(%C2%B7OH\)](https://www.membranechemicals.com/water-treatment/advanced-oxidation-plants/#:~:text=Advanced%20oxidation%20processes%20(abbreviation%3A%20AOPs,hydroxyl%20radicals%20(%C2%B7OH)) [Accessed: 30 June 2023].
- Bashir, M.J.K., Lim, J.H., Salem, Wong, L.M., and Sim, Y.L., 2019. Post treatment of palm oil mill effluent using electro-coagulation-peroxidation (ECP) technique. *Journal of Cleaner Production*, [e-journal] 208, pp. 716–727. <https://doi.org/10.1016/j.jclepro.2018.10.073>.
- Bashir, M.J.K., Wei, C.J., Aun, N.C. and Abu Amr, S.S., 2017. Electro persulphate oxidation for polishing of biologically treated palm oil mill effluent (POME). *Journal of Environmental Management*, [e-journal] 193, pp. 458–469. <https://doi.org/10.1016/j.jenvman.2017.02.031>.

- Behnajady, M.A., Modirshahla, N. and Shokri, M., 2004. Photo destruction of Acid Orange 7 (AO7) in aqueous solutions by UV/H₂O₂: influence of operational parameters. *Chemosphere*, [e-journal] 55, pp. 129–134. <https://doi.org/10.1016/j.chemosphere.2003.10.054>.
- Brillas, E., Sirés, I. and Oturan, M.A., 2009. Electro-Fenton process and related electrochemical technologies based on Fenton's reaction chemistry. *Chemical Reviews*, [e-journal] 109, pp. 6570–6631. <https://doi.org/10.1021/cr900136g>.
- Buthiyappan, A., Abdul Aziz, A.R. and Wan Daud, W.M.A., 2015. Degradation performance and cost implication of UV-integrated advanced oxidation processes for wastewater treatments. *Reviews in Chemical Engineering*, [e-journal] 31. <https://doi.org/10.1515/revce-2014-0039>.
- Cédat, B., de Brauer, C., Métivier, H., Dumont, N. and Tutundjan, R., 2016. Are UV photolysis and UV/H₂O₂ process efficient to treat estrogens in waters? Chemical and biological assessment at pilot scale. *Water Research*, [e-journal] 100, pp. 357–366. <https://doi.org/10.1016/j.watres.2016.05.040>.
- Chan, Y.J., Chong, M.F. and Law, C.L., 2012. Start-up, steady state performance and kinetic evaluation of a thermophilic integrated anaerobic–aerobic bioreactor (IAAB). *Bioresource Technology*, [e-journal] 125, pp. 145–157. <https://doi.org/10.1016/j.biortech.2012.08.118>.
- Choorit, W. and Wisarnwan, P., 2007. Effect of temperature on the anaerobic digestion of palm oil mill effluent. *Electronic Journal of Biotechnology*, [e-journal] 10. <https://doi.org/10.2225/vol10-issue3-fulltext-7>.
- Chu, W., Chan, K.H., Kwan, C.Y. and Choi, K.Y., 2007. Degradation of atrazine by modified stepwise-Fenton's processes. *Chemosphere*, [e-journal] 67, pp. 755–761. <https://doi.org/10.1016/j.chemosphere.2006.10.039>.
- Crittenden, J.C., Hu, S., Hand, D.J. and Green, S.A., 1999. A kinetic model for H₂O₂/UV process in a completely mixed batch reactor. *Water Research*, [e-journal] 33, pp. 2315–2328. [https://doi.org/10.1016/s0043-1354\(98\)00448-5](https://doi.org/10.1016/s0043-1354(98)00448-5).
- Cuerda-Correa, E.M., Alexandre-Franco, M.F. and Fernández-González, C., 2019. Advanced oxidation processes for the removal of antibiotics from water. An overview. *Water*, [e-journal] 12, p. 102. <https://doi.org/10.3390/w12010102>.
- Dakubo, F., Baygents, J.C. and Farrell, J., 2012. Hydrogen peroxide removal from chemical–mechanical planarization wastewater. *IEEE Transactions on Semiconductor Manufacturing*, [e-journal] 25, pp. 623–629. <https://doi.org/10.1109/tsm.2012.2205283>.

- Del Moro, G., Mancini, A., Mascolo, G. and Di Iaconi, C., 2013. Comparison of UV/H₂O₂ based AOP as an end treatment or integrated with biological degradation for treating landfill leachates. *Chemical Engineering Journal*, [e-journal] 218, pp. 133–137. <https://doi.org/10.1016/j.cej.2012.12.086>.
- Deng, Y. and Zhao, R., 2015. Advanced oxidation processes (AOPs) in wastewater treatment. *Current Pollution Reports*, [e-journal] 1, pp. 167–176. <https://doi.org/10.1007/s40726-015-0015-z>.
- Department of Environment (DOE), 1982. *Environment Quality Act 1974-Environment Quality (Prescribed Premises) (Crude Palm Oil) (Amendment) Regulations 1982*. [Online] Available from: [Peraturan_Kualiti_Alam_Sekeliling_Premis_Yang_Ditetapkan_Minyak_Kelapa_Sawit_Mentah_1977_-_P.U.A_342-77.pdf](https://www.doe.gov.my/images/stories/Peraturan_Kualiti_Alam_Sekeliling_Premis_Yang_Ditetapkan_Minyak_Kelapa_Sawit_Mentah_1977_-_P.U.A_342-77.pdf) (doe.gov.my) [Accessed 1st August 2023].
- Ebrahiem, E.E., Al-Maghrabi, Mohammednoor.N. and Mobarki, A.R., 2017. Removal of organic pollutants from industrial wastewater by applying photo-Fenton oxidation technology. *Arabian Journal of Chemistry*, [e-journal] 10, pp. S1674–S1679. <https://doi.org/10.1016/j.arabjc.2013.06.012>.
- Elfiana, E. and Fuadi, A., 2019. Advanced oxidation process using UV/H₂O₂ for organic substance removal in peat water based on discoloration signatures. *Proceedings of the 1st Workshop on Multidisciplinary and Its Applications Part 1, WMA-01 2018, 19-20 January 2018, Aceh, Indonesia* [e-journal]. <https://eudl.eu/pdf/10.4108/eai.20-1-2018.2281952>.
- Esplugas, S., Giménez, J., Contreras, S., Pascual, E. and RodríguezM., 2002. Comparison of different advanced oxidation processes for phenol degradation. *Water Research*, [e-journal] 36, pp. 1034–1042. [https://doi.org/10.1016/s0043-1354\(01\)00301-3](https://doi.org/10.1016/s0043-1354(01)00301-3).
- Gamaralalage, D., Sawai, O. and Nunoura, T., 2020. Effect of reagents addition method in Fenton oxidation on the destruction of organics in palm oil mill effluent. *Journal of Environmental Chemical Engineering*, [e-journal] 8, p. 103974. <https://doi.org/10.1016/j.jece.2020.103974>.
- Ghaly, M.Y., Georg Härtel, Mayer, R. and Haseneder, R., 2001. Photochemical oxidation of p-chlorophenol by UV/H₂O₂ and photo-Fenton process. *A comparative study. Waste Management (New York, N.Y.)*, [e-journal] 21, pp. 41–47. [https://doi.org/10.1016/s0956-053x\(00\)00070-2](https://doi.org/10.1016/s0956-053x(00)00070-2).
- Guinea, E., Arias, C., Cabot, P.L., José Luis Garrido, Rodríguez, R., Francesc Centellas and Enric Brillas, 2008. Mineralization of salicylic acid in acidic aqueous medium by electrochemical advanced oxidation processes using platinum and boron-doped diamond as anode and cathodically generated hydrogen peroxide. *Water Research*, [e-journal] 42, pp. 499–511. <https://doi.org/10.1016/j.watres.2007.07.046>.

- Gupta, N.K., Ghaffari, Y., Kim, S., Bae, J., Kim, K.S. and Saifuddin, M., 2020. Photocatalytic degradation of organic pollutants over MFe_2O_4 (M = Co, Ni, Cu, Zn) nanoparticles at neutral pH. *Scientific Reports*, [e-journal] 10. <https://doi.org/10.1038/s41598-020-61930-2>.
- H Movahedian, Mohammadi, S. and Asadi, A., 2009. Comparison of different advanced oxidation processes degrading p-chlorophenol in aqueous solution. *Iran. J. Environ. Health. Sci. Eng.*, [e-journal] 6, pp. 153–160.
- Hu, Q., Zhang, C., Wang, Z., Chen, Y., Ke-hui, M., Zhang Xingqing, Xiong, Y., and Zhu, M.J., 2008. Photodegradation of methyl tert-butyl ether (MTBE) by UV/H₂O₂ and UV/TiO₂. *Journal of Hazardous Materials*, [e-journal] 154, pp. 795–803. <https://doi.org/10.1016/j.jhazmat.2007.10.118>.
- Huang, C.P., Dong, C. and Tang, Z., 1993. Advanced chemical oxidation: Its present role and potential future in hazardous waste treatment. *Waste Management*, [e-journal] 13, pp. 361–377. [https://doi.org/10.1016/0956-053x\(93\)90070-d](https://doi.org/10.1016/0956-053x(93)90070-d).
- Huzir, N.M., Aziz, M.M.A., Ismail, S.B., Mahmood, N.A.N., Umor, N.A. and Faua'ad Syed Muhammad, S.A., 2019. Optimization of coagulation-flocculation process for the palm oil mill effluent treatment by using rice husk ash. *Industrial Crops and Products*, [e-journal] 139, p. 111482. <https://doi.org/10.1016/j.indcrop.2019.111482>.
- Iwuagwu, J.O. and Ugwuanyi, J.O. 2014. Treatment and valorization of palm oil mill effluent through production of food grade yeast biomass. *Journal of Waste Management*, [e-journal] 2014, pp. 1–9. <http://dx.doi.org/10.1155/2014/439071>.
- Julia, K.L., Munoz-Eraza, L. and Kemp, R.A., 2020. The intestinal tumour microenvironment. *Advances in Experimental Medicine and Biology*, [e-journal] pp. 1–22. https://doi.org/10.1007/978-3-030-36214-0_1.
- Kamyab, H., Chelliapan, S., Din, M.F.M., Rezania, S., Khademi, T. and Kumar, A., 2018. Palm oil mill effluent as an environmental pollutant. *Palm Oil*. [e-journal] <https://doi.org/10.5772/intechopen.75811>.
- Kim, M.J. and Nriagu, J., 2000. Oxidation of arsenite in groundwater using ozone and oxygen. *Science of The Total Environment*, [e-journal] 247, pp. 71–79. [https://doi.org/10.1016/S0048-9697\(99\)00470-2](https://doi.org/10.1016/S0048-9697(99)00470-2).
- Krishnan, S., Rawindran, H., Sinnathambi, C.M. and Lim, J.W., 2017. Comparison of various advanced oxidation processes used in remediation of industrial wastewater laden with recalcitrant pollutants. *IOP Conference Series: Materials Science and Engineering*, [e-journal] 206, p. 012089. <https://doi.org/10.1088/1757-899x/206/1/012089>.

- Ku, Y., Tu, Y.-H., and Ma, C.M., 2005. Effect of hydrogen peroxide on the decomposition of monochlorophenols by sonolysis in aqueous solution. *Water Research*, [e-journal] 39, pp. 1093–1098. <https://doi.org/10.1016/j.watres.2004.11.036>.
- Kusic, H., Koprivanac, N., Horvat, S., Bakija, S. and Bozic, A.L., 2009. Modelling dye degradation kinetic using dark- and photo-Fenton type processes. *Chemical Engineering Journal*, [e-journal] 155, pp. 144–154. <https://doi.org/10.1016/j.cej.2009.07.029>.
- Latif Ahmad, A., Ismail, S. and Bhatia, S., 2003. Water recycling from palm oil mill effluent (POME) using membrane technology. *Desalination*, [e-journal] 157, pp. 87–95. [https://doi.org/10.1016/s0011-9164\(03\)00387-4](https://doi.org/10.1016/s0011-9164(03)00387-4).
- Legrini, O., Oliveros, E. and Braun, A.M., 1993. Photochemical processes for water treatment. *Chemical Reviews*, [e-journal] 93, pp. 671–698. <https://doi.org/10.1021/cr00018a003>.
- Lescano, M., Zalazar, C., Cassano, A. and Brandi, R., 2012. Kinetic modelling of arsenic (III) oxidation in water employing the UV/H₂O₂ process. *Chemical Engineering Journal*, [e-journal] 211-212, pp. 360–368. <https://doi.org/10.1016/j.cej.2012.09.075>.
- Li, W., Jain, T., Ishida, K. and Liu, H., 2017. A mechanistic understanding of the degradation of trace organic contaminants by UV/hydrogen peroxide, UV/persulfate and UV/free chlorine for water reuse. *Environmental Science: Water Research & Technology*, [e-journal] 3, pp. 128–138. <https://doi.org/10.1039/c6ew00242k>.
- Litter, M. I., 2005. Introduction to photochemical advanced oxidation processes for water treatment. *Environmental Photochemistry Part II*, [e-journal] 2, pp. 325–366. <https://doi.org/10.1007/b138188>.
- Loh, S.K., Lai, M.E., Ngatiman, M., Lim, W.S., Choo, Y.M., Zhang, Z.J., Salimon, J., 2013. Zero discharge treatment technology of palm oil mill effluent. *Journal of Oil Palm Research*, [e-journal] 25, pp. 273-281. jopr.v25dec2013-soh1.pdf (mpob.gov.my).
- Lokman, N.A., Ahmad Muhsin Ithnin, Muhammad Nashren Ramli, Nadia Dayana Bahar, and Wira Jazair Yahya, 2019. Effect of filtered palm oil mill effluent (POME) via close loop in-line microbubbles treatment chamber for biochemical oxygen demand (BOD) treatment. *Journal of Advanced Research in Fluid Mechanics and Thermal Sciences*, [e-journal] 62, pp. 10-19. https://www.akademiabaru.com/doc/ARFMTSV62_N1_P10_19.pdf.

- López Cisneros, R., Gutarra Espinoza, A. and Litter, M.I., 2002. Photodegradation of an azo dye of the textile industry. *Chemosphere*, [e-journal] 48, pp. 393–399. [https://doi.org/10.1016/s0045-6535\(02\)00117-0](https://doi.org/10.1016/s0045-6535(02)00117-0).
- López, J.L., García, F.S., Gonzalez, M.C., Capparelli, A.L., Oliveros, E., Hashem, T. and Braun, A.M., 2000. Hydroxyl radical initiated photodegradation of 4-chloro-3,5-dinitrobenzoic acid in aqueous solution. *Journal of Photochemistry and Photobiology A-chemistry*, [e-journal] 37, pp. 177–184. [https://doi.org/10.1016/s1010-6030\(00\)00357-9](https://doi.org/10.1016/s1010-6030(00)00357-9).
- Luna, A.J., Nascimento, C.A.O. and Chiavone-Filho, O., 2006. Photodecomposition of hydrogen peroxide in highly saline aqueous medium. *Brazilian Journal of Chemical Engineering*, [e-journal] 23, pp. 341–349. <https://doi.org/10.1590/s0104-66322006000300007>.
- Ma, A.N. and Ong, A.S., 1985. Pollution Control in palm oil mills in Malaysia. *Journal of the American Oil Chemists' Society*, [e-journal] 62, pp. 261–266. <https://doi.org/10.1007/bf02541389>.
- Macawile, M.C., Centeno, C., Abella, L., Gallardo, S. and Suzuki, M., 2011. Effect of light intensity on the photodegradation of PCB 153 in aqueous solution using UV and UV/H₂O₂. *Journal of Water and Environment Technology*, [e-journal] 9, pp. 69–77. <https://doi.org/10.2965/jwet.2011.69>.
- Madaki, Y.S. and Seng, Lau., 2013. Palm oil mill effluent (POME) from Malaysia palm oil mills: Waste or resource. *International Journal of Science, Environment and Technology*, [e-journal] 2, pp. 1138-1155.
- Martínez, D.M., Ebenhack, B.W. and Wagner, T.P., 2019. Electric power sector energy efficiency. *Energy Efficiency*, [e-journal], pp. 129–160. <https://doi.org/10.1016/b978-0-12-812111-5.00005-6>.
- Meena R, A.A., J, M., Banu J, R., Bhatia, S.K., Kumar, V., Piechota, G. and Kumar, G., 2023. A review on the pollution assessment of hazardous materials and the resultant biorefinery products in Palm oil mill effluent. *Environmental Pollution*, [e-journal] 328, p. 121525. <https://doi.org/10.1016/j.envpol.2023.121525>.
- Mierzwa, J.C., Rodrigues, R. and Carlos, A., 2018. UV-hydrogen peroxide processes. *Elsevier eBooks*, [e-journal] pp. 13–48. <https://doi.org/10.1016/b978-0-12-810499-6.00002-4>.
- Miklos, D.B., Remy, C., Jekel, M., Linden, K.G., Drewes, J.E. and Hübner, U., 2018. Evaluation of advanced oxidation processes for water and wastewater treatment – A critical review. *Water Research*, [e-journal] 139, pp. 118–131. <https://doi.org/10.1016/j.watres.2018.03.042>.

- Modirshahla, N. and Behnajady, M.A., 2006. Photooxidative degradation of Malachite Green (MG) by UV/H₂O₂: Influence of operational parameters and kinetic modelling. *Dyes and Pigments*, [e-journal] 70, pp. 54–59. <https://doi.org/10.1016/j.dyepig.2005.04.012>.
- Mohammad, S., Baidurah, S., Kobayashi, T., Ismail, N. and Leh, C.P., 2021. Palm oil mill effluent treatment processes—A review. *Processes*, [e-journal] 9, p. 739. <https://doi.org/10.3390/pr9050739>.
- Mohammadi, P., Ibrahim, S., Annuar, M.S.M., Khashij, M., Mousavi, S.A. and Zinatizadeh, A., 2017. Optimization of fermentative hydrogen production from palm oil mill effluent in an up-flow anaerobic sludge blanket fixed film bioreactor. *Sustainable Environment Research*, [e-journal] 27, pp. 238–244. <https://doi.org/10.1016/j.serj.2016.04.015>.
- Mohammed Haji Alhaji, Khairuddin Sanaullah, Shanti Faridah Salleh, Rubiyah Baini, Soh Fong Lim, Ragai, A., Anwar, K. and Khan, A., 2018. Photo-oxidation of pre-treated palm oil mill Effluent using cylindrical column immobilized photoreactor. *Chemical Engineering Research & Design*, [e-journal] 117, pp. 180–189. <https://doi.org/10.1016/j.psep.2018.04.012>.
- Mohammed, N.A.A., I. Alwared, A., and S. Salman, M., 2020. Decolorization of reactive yellow dye by advanced oxidation using continuous reactors. *Iraqi journal of chemical and petroleum engineering*, [e-journal] 21, pp. 1–6. <https://doi.org/10.31699/ijcpe.2020.2.1>.
- Mohammed, R.R., and Chong, M.F., 2014. Treatment and decolorization of biologically treated palm oil mill effluent (POME) using banana peel as novel biosorbent. *Journal of Environmental Management*, [e-journal] 132, pp. 237–249. <https://doi.org/10.1016/j.jenvman.2013.11.031>.
- Monteagudo, J.M., A. Durán, I. San Martín and Aguirre, M., 2009. Effect of continuous addition of H₂O₂ and air injection on ferrioxalate-assisted solar photo-Fenton degradation of Orange II. *Applied Catalysis B-environmental*, [e-journal] 89, pp. 510–518. <https://doi.org/10.1016/j.apcatb.2009.01.008>.
- Morgan, M.S., Van Trieste, P.F., Garlick, S.M., Mahon, M.J. and Smith, A.L., 1988. Ultraviolet molar absorptivities of aqueous hydrogen peroxide and hydroperoxyl ion. *Analytica Chimica Acta*, [e-journal] 215, pp. 325–329. [https://doi.org/10.1016/s0003-2670\(00\)85294-0](https://doi.org/10.1016/s0003-2670(00)85294-0).
- Munter, R., 2001. Advanced oxidation processes – current status and prospects. Proceedings of the Estonian academy of sciences. *Chemistry*, [e-journal] 50, p. 59. <https://doi.org/10.3176/chem.2001.2.01>.

- Muruganandham, M. and Swaminathan, M., 2004. Photochemical oxidation of reactive azo dye with UV/H₂O₂ process. *Dyes and Pigments*, [e-journal] 62, pp. 269–275. <https://doi.org/10.1016/j.dyepig.2003.12.006>.
- Muruganandham, M. and Swaminathan, M., 2006. Advanced oxidative decolourisation of Reactive Yellow 14 azo dye by UV/TiO₂, UV/H₂O₂, UV/H₂O₂/Fe²⁺ processes—a comparative study. *Separation and Purification Technology*, [e-journal] 48, pp. 297–303. <https://doi.org/10.1016/j.seppur.2005.07.036>.
- Neyens, E. and Baeyens, J., 2003. A review of classic Fenton's peroxidation as an advanced oxidation technique. *Journal of Hazardous Materials*, [e-journal] 98, pp. 33–50. [https://doi.org/10.1016/s0304-3894\(02\)00282-0](https://doi.org/10.1016/s0304-3894(02)00282-0).
- Nogueira, V., Lopes, I., Rocha-Santos, T.A.P., Gonçalves, F., Duarte, A.C. and Pereira, R., 2016. Photocatalytic treatment of olive oil mill wastewater using TiO₂ and Fe₂O₃ nanomaterials. *Water, Air, & Soil Pollution*, [e-journal] 227. <https://doi.org/10.1007/s11270-016-2787-1>.
- O'Shea, K.E. and Dionysiou, D.D., 2012. Advanced oxidation processes for water treatment. *The Journal of Physical Chemistry Letters*, [e-journal] 3, pp. 2112–2113. <https://doi.org/10.1021/jz300929x>.
- Osman, N.A., Ujang, F.A., Roslan, A.M., Ibrahim, M.F. and Hassan, M.A., 2020. The effect of palm oil mill effluent final discharge on the characteristics of *Pennisetum purpureum*. *Scientific Reports*, [e-journal] 10, pp. 1–10. <https://doi.org/10.1038/s41598-020-62815-0>.
- Oswal, N., Sarma, P.M., Zinjarde, S.S. and Pant, A., 2002. Palm oil mill effluent treatment by a tropical marine yeast. *Bioresource Technology*, [e-journal] 85, pp. 35–37. [https://doi.org/10.1016/s0960-8524\(02\)00063-9](https://doi.org/10.1016/s0960-8524(02)00063-9).
- Oturan, M.A. and Aaron, J.J., 2014. Advanced oxidation processes in water/wastewater treatment: Principles and applications. A Review. *Critical Reviews in Environmental Science and Technology*, [e-journal] 44, pp. 2577–2641. <https://doi.org/10.1080/10643389.2013.829765>.
- Parsons, S., 2015. Advanced oxidation processes for water and wastewater treatment. *Water Intelligence Online*, [e-journal] 4, p. 9781780403076-9781780403076. <https://doi.org/10.2166/9781780403076>.
- Parthasarathy, S., Gomes, R.L. and Manickam, S., 2015. Process intensification of anaerobically digested palm oil mill effluent (AAD-POME) treatment using combined chitosan coagulation, hydrogen peroxide (H₂O₂) and Fenton's oxidation. *Clean Technologies and Environmental Policy*, [e-journal] 18, pp. 219–230. <https://doi.org/10.1007/s10098-015-1009-7>.

- Parveez, A., 2023. Oil palm economic performance in Malaysia and R&D progress in 2022. *Journal of Oil Palm Research*, [e-journal] 35. <https://doi.org/10.21894/jopr.2023.0028>.
- Pera-Titus, M., García-Molina V., Baños, M.A., Giménez, J. and Esplugas, S., 2004. Degradation of chlorophenols by means of advanced oxidation processes: A general review. *Applied Catalysis B: Environmental*, [e-journal] 47, pp. 219–256. <https://doi.org/10.1016/j.apcatb.2003.09.010>.
- Pérez-Sicairos, S., Corrales-López, K.A., Hernández-Calderón, Ó.M., Salazar-Gastélum, M.I. and Félix-Navarro, R.M., 2016. Photochemical degradation of nitrobenzene by $S_2O_8^{2-}$ ions and UV radiation. *Revista Internacional de Contaminación Ambiental*, [e-journal] 32, pp. 227–236. <https://doi.org/10.20937/rica.2016.32.02.08>.
- Pettine, M., Campanella, L. and Millero, F.J., 1999. Arsenite oxidation by H_2O_2 in aqueous solutions. *Geochimica et Cosmochimica Acta*, [e-journal] 63, pp. 2727–2735. [https://doi.org/10.1016/s0016-7037\(99\)00212-4](https://doi.org/10.1016/s0016-7037(99)00212-4).
- Pham Minh, D., Siang, T.J., Vo, D.V.N., Phan, T.S., Ridart, C., Nzihou, A. and Grouset, D., 2018. Hydrogen production from biogas reforming: An overview of steam reforming, dry reforming, dual reforming, and tri-reforming of methane. *Hydrogen Supply Chains*, [e-journal] pp. 111–166. <https://doi.org/10.1016/b978-0-12-811197-0.00004-x>.
- Phang, Y.K., Aminuzzaman, M., Akhtaruzzaman, Md., Muhammad, G., Ogawa, S., Watanabe, A. and Tey, L.H., 2021. Green synthesis and characterization of CuO nanoparticles derived from papaya peel extract for the photocatalytic degradation of palm oil mill effluent (POME). *Sustainability*, [e-journal] 13, p. 796. <https://doi.org/10.3390/su13020796>.
- Poh, P.E., and Chong, M.F., 2014. Upflow anaerobic sludge blanket-hollow centered packed bed (UASB-HCPB) reactor for thermophilic palm oil mill effluent (POME) treatment. *Biomass and Bioenergy*, [e-journal] 67, pp. 231–242. <https://doi.org/10.1016/j.biombioe.2014.05.007>.
- Prasertsan, S. and Prasertsan, P., 1996. Biomass residues from palm oil mills in Thailand: An overview on quantity and potential usage. *Biomass and Bioenergy*, [e-journal] 11, pp. 387–395. [https://doi.org/10.1016/S0961-9534\(96\)00034-7](https://doi.org/10.1016/S0961-9534(96)00034-7).
- Prato-Garcia, D. and Buitrón, G., 2012. Evaluation of three reagent dosing strategies in a photo-fenton process for the decolorization of azo dye mixtures. *Journal of Hazardous Materials*, [e-journal] 217–218, pp. 293–300. <https://doi.org/10.1016/j.jhazmat.2012.03.036>.

- Prieto-Rodríguez, L., Oller, I., Zapata, A., Agüera, A. and Malato, S., 2011. Hydrogen peroxide automatic dosing based on dissolved oxygen concentration during solar photo-Fenton. *Catalysis Today*, [e-journal] 161, pp. 247–254. <https://doi.org/10.1016/j.cattod.2010.11.017>.
- Primo, O., Rivero, M.J., Ortiz, I. and Irabien, A., 2007. Mathematical modelling of phenol photooxidation: Kinetics of the process toxicity. *Chemical Engineering Journal*, [e-journal] 134, pp. 23–28. <https://doi.org/10.1016/j.cej.2007.03.061>.
- Reisz, E., Schmidt, W., Schuchmann, H.P. and C., von Sonntag, 2003. Photolysis of ozone in aqueous solutions in the presence of tertiary butanol. *Environmental Science & Technology*, [e-journal] 37, pp. 1941–1948. <https://doi.org/10.1021/es0113100>.
- Saleh, A.F., E. Kamarudin, Yaacob, A.B., Yussof, A.W., and Mohd Zulkifly Abdullah, 2012. Optimization of biomethane production by anaerobic digestion of palm oil mill effluent using response surface methodology. *Asia-Pacific Journal of Chemical Engineering*, [e-journal] 7, pp. 353–360. <https://doi.org/10.1002/apj.550>.
- Saravanan, A., Deivayanai, V.C., Kumar, P.S., Rangasamy, G., Hemavathy, R.V., Harshana, T., Gayathri, N. and Alagumalai, K., 2022. A detailed review on advanced oxidation process in treatment of wastewater: Mechanism, challenges, and future outlook. *Chemosphere*, [e-journal] 308, p. 136524. <https://doi.org/10.1016/j.chemosphere.2022.136524>.
- Shu, H.Y. and Chang, M.C., 2005. Decolorization and mineralization of a phthalocyanine dye C.I. Direct Blue 199 using UV/H₂O₂ process. *Journal of Hazardous Materials*, [e-journal] 125, pp. 96–101. <https://doi.org/10.1016/j.jhazmat.2005.05.016>.
- Silva, A.M.T., Nouli, E., Xekoukoulotakis, N.P. and Mantzavinos, D., 2007. Effect of key operating parameters on phenols degradation during H₂O₂-assisted TiO₂ photocatalytic treatment of simulated and actual olive mill wastewaters. *Applied Catalysis B: Environmental*, [e-journal] 73, pp. 11–22. <https://doi.org/10.1016/j.apcatb.2006.12.007>.
- Sohn, J.H., Kwon, K.K., Kang, J.H., Jung, H.B. and Kim, S.J., 2004. *Novosphingobium pentaromativorans* sp. nov., a high-molecular-mass polycyclic aromatic hydrocarbon-degrading bacterium isolated from estuarine sediment. *International Journal of Systematic and Evolutionary Microbiology*, [e-journal] 54, pp. 1483–1487. <https://doi.org/10.1099/ijs.0.02945-0>.
- Soleimaninanadegani, M. and Manshad, S., 2014. Enhancement of biodegradation of palm oil mill effluents by local isolated microorganisms. *International Scholarly Research Notices*, [e-journal] 2014, pp. 1–8. <https://doi.org/10.1155/2014/727049>.

- Sujatha, G., Shanthakumar, S. and Chiampo, F., 2020. UV light-irradiated photocatalytic degradation of coffee processing wastewater using TiO₂ as a catalyst. *Environments*, [e-journal] 7, p. 47. <https://doi.org/10.3390/environments7060047>.
- Sun, W., Dong, H., Wang, Y., Duan, S., Ji, W., Huang, H., Gu, J. and Qiang, Z., 2023. Ultraviolet (UV)-based advanced oxidation processes for micropollutant abatement in water treatment: gains and problems. *Journal of Environmental Chemical Engineering*, [e-journal] 11, pp. 110425–110425. <https://doi.org/10.1016/j.jece.2023.110425>.
- Tamrin, K.F. and Zahrim, A.Y., 2016. Determination of optimum polymeric coagulant in palm oil mill effluent coagulation using multiple-objective optimisation on the basis of ratio analysis (Moora). *Environmental Science and Pollution Research*, [e-journal] 24, pp. 15863–15869. <https://doi.org/10.1007/s11356-016-8235-3>.
- Tokumura, M., Morito, R., Hatayama, R. and Kawase, Y., 2011. Iron redox cycling in hydroxyl radical generation during the photo-Fenton oxidative degradation: Dynamic change of hydroxyl radical concentration. *Applied Catalysis B: Environmental*, [e-journal] 106, pp. 565–576. <https://doi.org/10.1016/j.apcatb.2011.06.017>.
- Urbina-Suarez, N.A., López-Barrera, G.L., García-Martínez, J.B., Barajas-Solano, A.F., Machuca-Martínez, F. and Zuorro, A., 2023. Enhanced UV/H₂O₂ system for the oxidation of organic contaminants and ammonia transformation from tannery effluents. *Processes*, [e-journal] 11, p. 3091. <https://doi.org/10.3390/pr11113091>.
- Verma, N. and Singh, A.K., 2013. Development of biological oxygen demand biosensor for monitoring the fermentation industry effluent. *ISRN Biotechnology*, [e-journal] 2013, pp. 1–6. <https://doi.org/10.5402/2013/236062>.
- Vinge, S.L., Rosenblum, J.S., Linden, Y.S., Saenz, A., Hull, N.M., and Linden, K.G., 2021. Assessment of UV disinfection and advanced oxidation processes for treatment and reuse of hydraulic fracturing produced water. *ACS ES&T Engineering*, [e-journal] 1, pp. 490–500. <https://doi.org/10.1021/acsestengg.0c00170>.
- von Sonntag, C., 2008. Advanced oxidation processes: Mechanistic aspects. *Water Science and Technology*, [e-journal] 58, pp. 1015–1021. <https://doi.org/10.2166/wst.2008.467>.
- Wang, F., Zhang, L., Wei, L. and van der Hoek, J.P., 2021. Removal of hydrogen peroxide residuals and by-product bromate from advanced oxidation processes by granular activated carbon. *Water*, [e-journal] 13, p. 2460. <https://doi.org/10.3390/w13182460>.

- Wang, J., Mahmood, Q., Qiu, J.P., Li, Y.S., Chang, Y.S., Chi, L.N. and Li, X.D., 2015. Zero discharge performance of an industrial pilot-scale plant treating palm oil mill effluent. *BioMed Research International*, [e-journal] 2015, pp. 1–9. <https://doi.org/10.1155/2015/617861>.
- Wang, J.L. and Xu, L.J., 2012. Advanced oxidation processes for wastewater treatment: Formation of hydroxyl radical and application. *Critical Reviews in Environmental Science and Technology*, [e-journal] 42, pp. 251–325. <https://doi.org/10.1080/10643389.2010.507698>.
- Wang, Y., Guo, C., Sun, F., Shen, Z. and Guo, D., 2011. Dynamic neural-fuzzified adaptive control of ship course with parametric modelling uncertainties. *International Journal of Modelling, Identification and Control*, [e-journal] 13, p. 251. <https://doi.org/10.1504/ijmic.2011.041780>.
- Wong, K.A., Lam, S.M. and Sin, J.C., 2019. Wet chemically synthesized ZnO structures for photodegradation of pre-treated palm oil mill effluent and antibacterial activity. *Ceramics International*, [e-journal] 45, pp. 868–1880. <https://doi.org/10.1016/j.ceramint.2018.10.078>.
- Wu, T. and Englehardt, J.D., 2012. A new method for removal of hydrogen peroxide interference in the analysis of chemical oxygen demand. *Environmental Science & Technology*, [e-journal] 46, pp. 2291–2298. <https://doi.org/10.1021/es204250k>.
- Wu, T.Y., Mohammad, A.W., Md. Jahim, J. and Anuar, N., 2007. Palm oil mill effluent (POME) treatment and bioresources recovery using ultrafiltration membrane: Effect of pressure on membrane fouling. *Biochemical Engineering Journal*, [e-journal] 35, pp. 309–317. <https://doi.org/10.1016/j.bej.2007.01.029>.
- Xiang, Y., Gonsior, M., Philippe Schmitt-Kopplin and Shang, C., 2020. Influence of the UV/H₂O₂ advanced oxidation process on dissolved organic matter and the connection between elemental composition and disinfection byproduct formation. *Environmental Science & Technology*, [e-journal] 54, pp. 14964–14973. <https://doi.org/10.1021/acs.est.0c03220>.
- Yao, H., Sun, P., Minakata, D., Crittenden, J.C., and Huang, C.H., 2013. Kinetics and modelling of degradation of ionophore antibiotics by UV and UV/H₂O₂. *Environmental Science & Technology*, [e-journal] 47, pp. 4581–4589. <https://doi.org/10.1021/es3052685>.
- Yashni, G., Al-Gheethi, A., Radin Mohamed, R.M.S., Arifin, S.N.H. and Mohd Salleh, S.N.A., 2020. Conventional and advanced treatment technologies for palm oil mill effluents: a systematic literature review. *Journal of Dispersion Science and Technology*, [e-journal] 42, pp. 1766–1784. <https://doi.org/10.1080/01932691.2020.1788950>.

- Yu, L., Iranmanesh, S., Keir, I. and Achari, G., 2020. A field pilot study on treating groundwater contaminated with sulfolane using UV/H₂O₂. *Water*, [e-journal] 12, p. 1200. <https://doi.org/10.3390/w12041200>.
- Yu, X., Moisès Graells, S. Miralles-Cuevas, Cabrera-Reina, A., and Montserrat Pérez-Moya, 2021. An improved hybrid strategy for online dosage of hydrogen peroxide in photo-Fenton processes. *Journal of Environmental Chemical Engineering*, [e-journal] 9, pp. 105235–105235. <https://doi.org/10.1016/j.jece.2021.105235>.
- Yu, X., Somoza-Tornos, A., Graells, M. and Pérez-Moya, M., 2020. An experimental approach to the optimization of the dosage of hydrogen peroxide for Fenton and photo-Fenton processes. *Science of The Total Environment*, [e-journal] 743, p. 140402. <https://doi.org/10.1016/j.scitotenv.2020.140402>.
- Zainal, N.H., 2018. A review on the development of palm oil mill effluent (POME) final discharge polishing treatments. *Journal of Oil Palm Research*, [e-journal] 29, pp. 528–540. <https://doi.org/10.21894/jopr.2017.00012>.
- Zainal, N.H., Aziz, A.A., Idris, J., Jalani, N.F., Mamat, R., Ibrahim, M.F., Hassan, M.A. and Abd-Aziz, S., 2018. Reduction of POME final discharge residual using activated bioadsorbent from oil palm kernel shell. *Journal of Cleaner Production*, [e-journal] 182, pp. 830–837. <https://doi.org/10.1016/j.jclepro.2018.02.110>.
- Zainuri, N.Z., Hairom, N.H.H., Sidik, D.A.B., Desa, A.L., Misdan, N., Yusof, N. and Mohammad, A.W., 2018. Palm oil mill secondary effluent (POMSE) treatment via photocatalysis process in presence of ZnO-PEG nanoparticles. *Journal of Water Process Engineering*, [e-journal] 26, pp. 10–16. <https://doi.org/10.1016/j.jwpe.2018.08.009>.
- Zang, Y. and Farnood, R., 2005. Effects of hydrogen peroxide concentration and ultraviolet light intensity on methyl tert-butyl ether degradation kinetics. *Chemical Engineering Science*, [e-journal] 60, pp. 1641–1648. <https://doi.org/10.1016/j.ces.2004.11.003>.
- Zazo, J.A., Casas, J.A., Mohedano, A.F. and Rodriguez, J.J., 2009. Semicontinuous Fenton oxidation of phenol in aqueous solution. A kinetic study. *Water Research*, [e-journal] 43, pp. 4063–4069. <https://doi.org/10.1016/j.watres.2009.06.035>.
- Zhang, Y., Yan, L., Qiao, X., Hamidreza Arandiyani, Niu, X., Mei, Z. and Zhang, Z., 2008. Integration of biological method and membrane technology in treating palm oil mill effluent. *Journal of Environmental Sciences*, [e-journal] 20, pp. 558–564. [https://doi.org/10.1016/s1001-0742\(08\)62094-x](https://doi.org/10.1016/s1001-0742(08)62094-x).

- Zinatizadeh, A.A., Ibrahim, S., Aghamohammadi, N., Mohamed, A.R., Zangeneh, H. and Mohammadi, P., 2016. Polyacrylamide-induced coagulation process removing suspended solids from palm oil mill effluent. *Separation Science and Technology*, [e-journal] 52, pp. 520–527. <https://doi.org/10.1080/01496395.2016.1260589>.
- Zinatizadeh, A.A.L., Mohamed, A.R., Abdullah, A.Z., Mashitah, M.D., Hasnain Isa, M. and Najafpour, G.D., 2006. Process modelling and analysis of palm oil mill effluent treatment in an up-flow anaerobic sludge fixed film bioreactor using response surface methodology (RSM). *Water Research*, [e-journal] 40, pp. 3193–3208. <https://doi.org/10.1016/j.watres.2006.07.005>.
- Zoschke, K., Dietrich, N., Börnick, H. and Worch, E., 2012. UV-based advanced oxidation processes for the treatment of odour compounds: Efficiency and by-product formation. *Water Research*, [e-journal] 46, pp. 5365–5373. <https://doi.org/10.1016/j.watres.2012.07.012>.